

Whisker Growth and Cavity Formation at the Microscale

Leonid M. Dorogin¹, Maksim V. Dorogov¹, Sergei Vlassov^{1,2}, Anatoly A. Vikarchuk³ and Alexey E. Romanov¹

¹ITMO University, Kronverkskiy 49, 197101 Saint-Petersburg, Russia

²Institute of Physics, University of Tartu, W. Ostwaldi str. 1, 50411 Tartu, Estonia

³Togliatti State University, Belorusskaya str. 14, 445020 Togliatti, Russia

Received: March 09, 2020

Abstract. We discuss a recent progress in research on micro-/nanoscale metal and oxide whiskers. It is common to define whiskers as quasi-one-dimensional (elongated) solid objects that formed on a surface of a crystalline material by growth from its base. Whisker growth is often accompanied by formation of cavities and cracks in the bulk of material. This fact did facilitate the advancing of various explanations on the mass transfer for whisker growth. First theoretical models of metal whiskers growth were based on the theory of crystal lattice defects and on the assumption of inherent mechanical stresses in the material that “push” the whisker out. However, those models were not applicable to all variety of whisker growth observed. There are more complex cases of whiskers, such as oxide whiskers that formed in chemical reactions, such as oxidation during annealing in air or a synthetic reaction in a liquid. Theoretical modelling of the complex cases is still a challenging task at the border of chemical kinetics and materials science. Oxide whiskers are usually considered separately from metal whiskers, thus the fundamental interlink between the two cases might be lost. The goal of the present review is to collect the most prominent observations and theoretical explanations of whisker growth for both single phase and compound objects into a single document.

1. INTRODUCTION

Whiskers are quasi-one-dimensional (1D) solid structures of diameters ranging from several tens nanometers (nm) to several microns (μm) and reaching values of the order of several millimeters (mm) in their length, often observed on surfaces of crystalline solids, such as metals as well as some other materials. Whiskers on galvanic cadmium (Cd) coatings have been discovered since the 1940s [1]. Further, whiskers on tin (Sn) coatings have been described in the literature (see, for example, [2,3]). Such whiskers grew, in particular, on the contacts of electronic components and capacitor plates, causing a malfunction in their operation due to short circuits.

Tin whiskers are a serious problem for electronics of all types (Fig. 1a). They are almost invisible to a naked eye and 10-100 times thinner than human hair. Conductive whiskers grow on pure tin, when used as an exter-

nal layer for the terminals of electronic components. They can grow very quickly with a period of “incubation” from several days to several years.

Later it was found that the addition of lead (Pb) to tin inhibited the growth of whiskers. Since then, eutectic solder based on tin and lead has become the standard in the electronics industry until recently. In the 2000s, the EU adopted the RoHS (Restriction of Hazardous Substances) directive, which requires elimination of lead from electronic devices. Now all the connectors, passive and active components, switches and relays should not contain lead. Thus, RoHS requirements created new challenges for the electronics industry, in particular, with respect to the problem of whisker growth.

In addition to the cadmium and tin whiskers, spontaneous growth of whiskers of other metals, such as zinc (Zn) and silver (Ag), is possible under certain conditions [2].

Corresponding author: L.M. Dorogin, e-mail: lmdorogin@itmo.ru

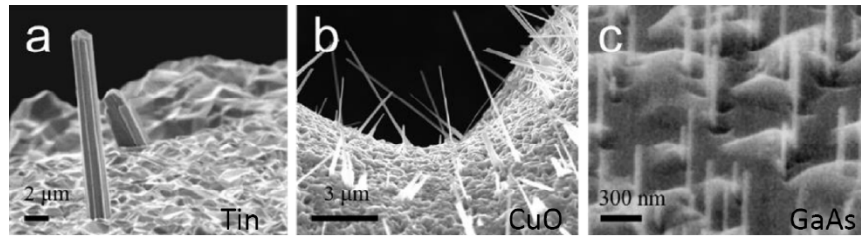


Fig. 1. Microscopic images of whiskers. (a) tin whiskers, adapted from [17], (b) CuO whiskers, (c) GaAs whiskers. Adapted from Ref. [16].

The presence of internal mechanical stresses was called one of the conditions for whiskers to grow [4]. It was also argued that high growth rate cannot be explained by bulk self-diffusion of atoms in the crystal and must involve much faster atomic transport mechanisms, such as grain boundary diffusion [5]. Rapid growth of silver whiskers from the nanoporous TiO_2 coating with embedded silver nanowires was observed inside the scanning electron microscope (SEM) under the electron beam [6]. The phenomenon observed in [6] is an example of an exceptional diffusion activated under electron beam irradiation, which still lacks a rigorous explanation.

Several concepts and models for whisker growth and cavity formation have been proposed using different approaches: dislocation models [7-11], recrystallization models [4], diffusion models [12]. In particular, prismatic dislocation loops have been considered as the carrier of mass transfer during whisker growth [9].

In addition to mechanical stresses, chemical reactions can also lead to the formation of whiskers and internal cavities in the oxide particles, as will be described later. One typical example is the growth of whiskers of copper oxide on the surface of copper foil (Fig. 1b) or copper microparticles when heated to 250-700 °C under conditions of access to oxygen [13,14]. Such phenomenon can be considered as a special mechanism of oxidation, which requires dedicated studies. Copper oxide whiskers had been actively investigated for industrial applications as a potential catalyst with a developed surface for the production of methanol or water purification [15]. As another example of non-metallic whiskers, we can point out semiconductor filamentary nanocrystals of GaAs growing on gold-activated surfaces [16] (Fig. 1c).

The information collected in this article provides a review of the results on whisker observation in various materials including metals and oxides and on theoretical models advanced for explanation of whisker growth in connection to mass-transfer processes in bulk of the material.

The review starts with a short introduction to the most typical cases of experimentally observed whiskers

in the Section 2, followed by a description of a select of analytical experimental studies of whisker growth and general physical factors of whisker growth in the Section 3. In the Section 4 some of the most prominent attempts to describe whisker growth theoretically in the framework of materials science are presented. In the Section 5 we call the attention to the whisker growth and cavity formation in small particles, where based on recent experimental results and theoretical interpretations we show how those two processes can be directly linked. Finally, we conclude on the whole topic of the review in the Section 6.

2. PROMINENT EXPERIMENTAL OBSERVATIONS OF WHISKER GROWTH

2.1. Metallic whiskers

Spontaneous growth of whiskers under ambient conditions was observed in the galvanic surfaces of many metals deposited on metal substrates, including:

- Tin (Fig. 2) [17];
- Cadmium;
- Zinc on a steel base [18];
- Bismuth in composite coatings [19].

In laboratory conditions, other types of metal whiskers can also be produced, such as:

- silver whiskers in the atmosphere of hydrogen sulfide H_2S [20];
- aluminum whiskers in a certain temperature range [21];
- copper whiskers on the surface of small copper particles [10,22] (Fig. 3).

2.2. Oxide and other non-metallic whiskers

The first literature data on oxide whiskers CuO appeared in the 1950s [23] and further continued in [14]. The synthesis of CuO whiskers is relatively simple and consists in controlled heating of the sample to certain temperatures in the presence of oxygen. Copper foil or a specially manufactured structured material can be used as an initial sample [24].

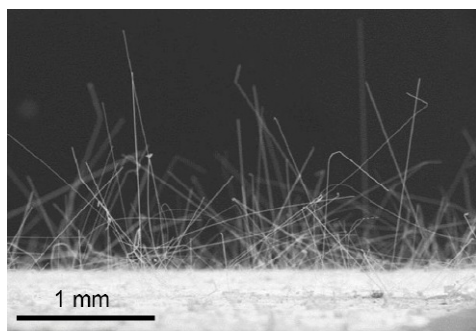


Fig. 2. SEM image of an array of tin whiskers. Adapted from Ref. [17].

It is worth noting separately the possibility to use small particles as a basis for growing oxide whiskers. The results of experimental studies of annealing of icosahedral small particles of copper obtained by electrodeposition are described in [25] (Fig. 4). An annealing was carried out in a vacuum oven at temperatures of 100-800 °C and in air at 300-600 °C. There the growth of whiskers was noticed only in experiments in air, which evidently indicates that the growth of CuO whiskers is a special type of copper oxidation.

Whiskers can also be produced in various chemical solutions at room temperature [26]. The synthesis of nanostructured copper-based films including fibers and “scrolls” of $\text{Cu}(\text{OH})_2$, whiskers and CuO plates, the array of rods $\text{Cu}_2(\text{OH})_2\text{CO}_3$ is studied in Ref. [26]. The films were obtained by oxidizing copper in aqueous so-

lutions of NaOH or NaHCO_3 with an oxidant $(\text{NH}_4)_2\text{S}_2\text{O}_8$. The authors emphasize that, despite the low-temperature synthesis regime, most of the resulting nanostructures are single crystals.

Here were listed only some of the basic methods for the synthesis of whiskers. A detailed review of the various types of synthesized non-metallic nanostructures can be found in [27].

3. ANALYTICAL EXPERIMENTAL STUDIES OF WHISKER GROWTH

3.1. Generalized factors of whisker growth

The growth of whiskers is a complex phenomenon, which depends on external conditions and the internal structure of the initial sample. Below are listed several main factors controlling the growth of whiskers and describing their properties.

1. The mechanism of growth whisker.
2. Temperature and external environment. Homological temperature of the sample material. Presence and portion pressure of reactive gases.
3. Internal structure of whiskers. Mono- or polycrystallinity. The presence of kinks, crystal lattice defects and branching.
4. The internal structure of the coating layer and the substrate. Grain structure, chemical composition, crystal lattice defects.

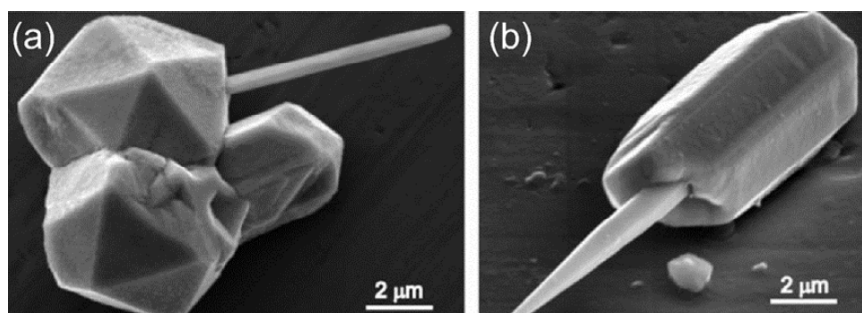


Fig. 3. Copper whiskers on copper particles obtained by electrodeposition. Reproduced with permission from Ref. [10].

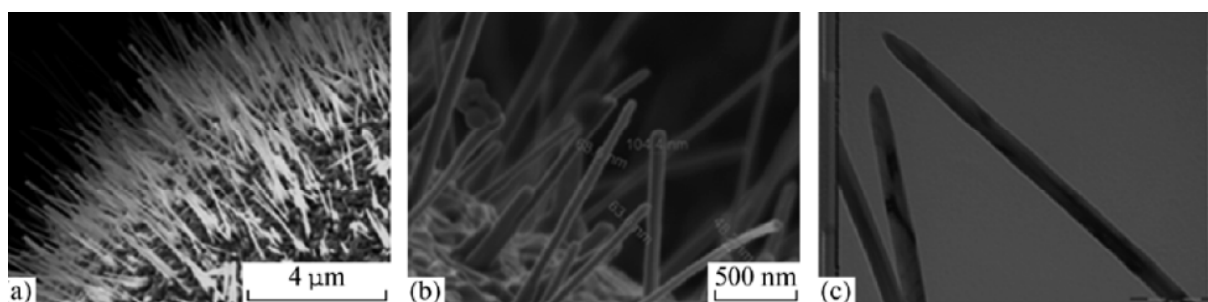


Fig. 4. Whiskers of CuO, obtained on the surface of small particles of copper during annealing in air. Reprinted by permission from Springer Nature Customer Service Centre GmbH : Springer Nature : JETP Letters Ref. [25], © 2013.

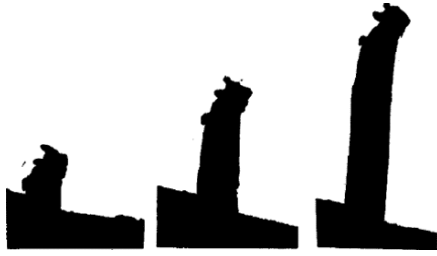


Fig. 5. Images of electron microscopy showing the growth stages of tin whiskers. Reprinted from [28], with the permission of AIP Publishing.

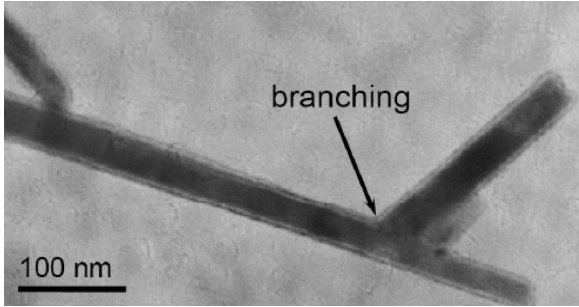


Fig. 6. Transmission electron microscopy (TEM) image of the CuO whisker branch. Adapted from Ref. [29].

5. Internal mechanical stresses of the coating layer and the substrate.

The following sections of this chapter will outline the main results of experimental studies on the growth of whiskers, aimed at elucidating the role of these main factors.

3.2. Mechanisms of whisker growth

An important characteristic of whiskers is the type of their growth. We can distinguish two main types of whisker growth:

- growth **out** from the base;
- growth **onto** the surface.

In the first case, the substance is transferred completely or partially from the surface layer to the base of the whisker. This type of growth is characteristic for metal whiskers of tin [28], cadmium, aluminium [21] and silver [20]. This was first concluded from observations of the successive phases of growth of a tin whisker in [28] (Fig. 5).

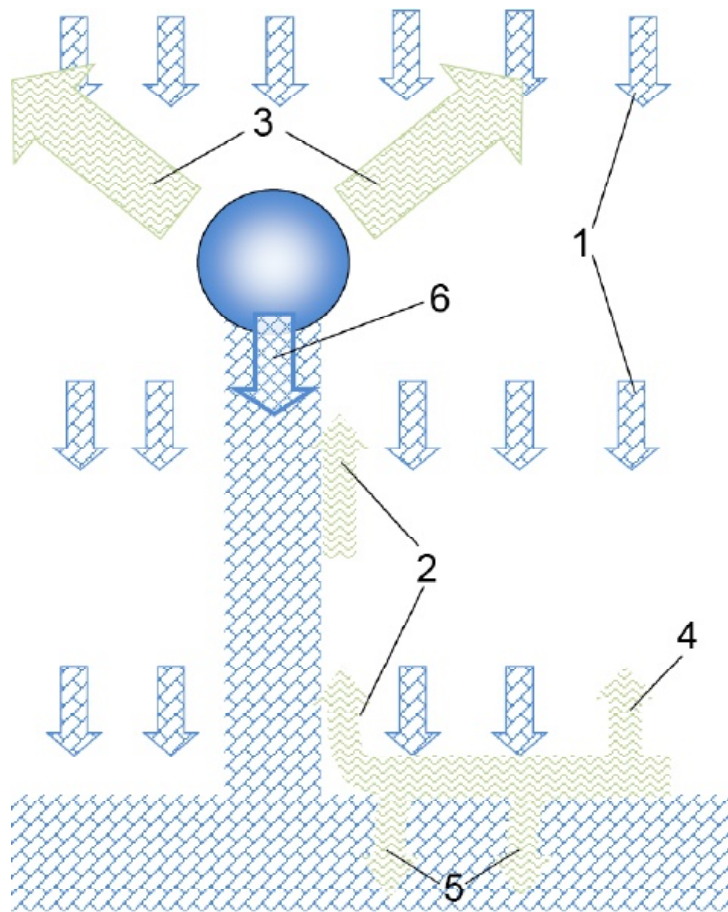


Fig. 7. Generalized scheme of whisker growth by the mechanism of vapor-liquid-crystal. Designations: 1 - molecular flow, delivering material to the drop and on the substrate, 2 - diffusion of adatoms from the surface to the drop, 3 - desorption from the droplet, 4 - desorption from the surface of the substrate, 5 - growth of the substrate, 6 - growth of the whisker. Adapted from Ref. [16].

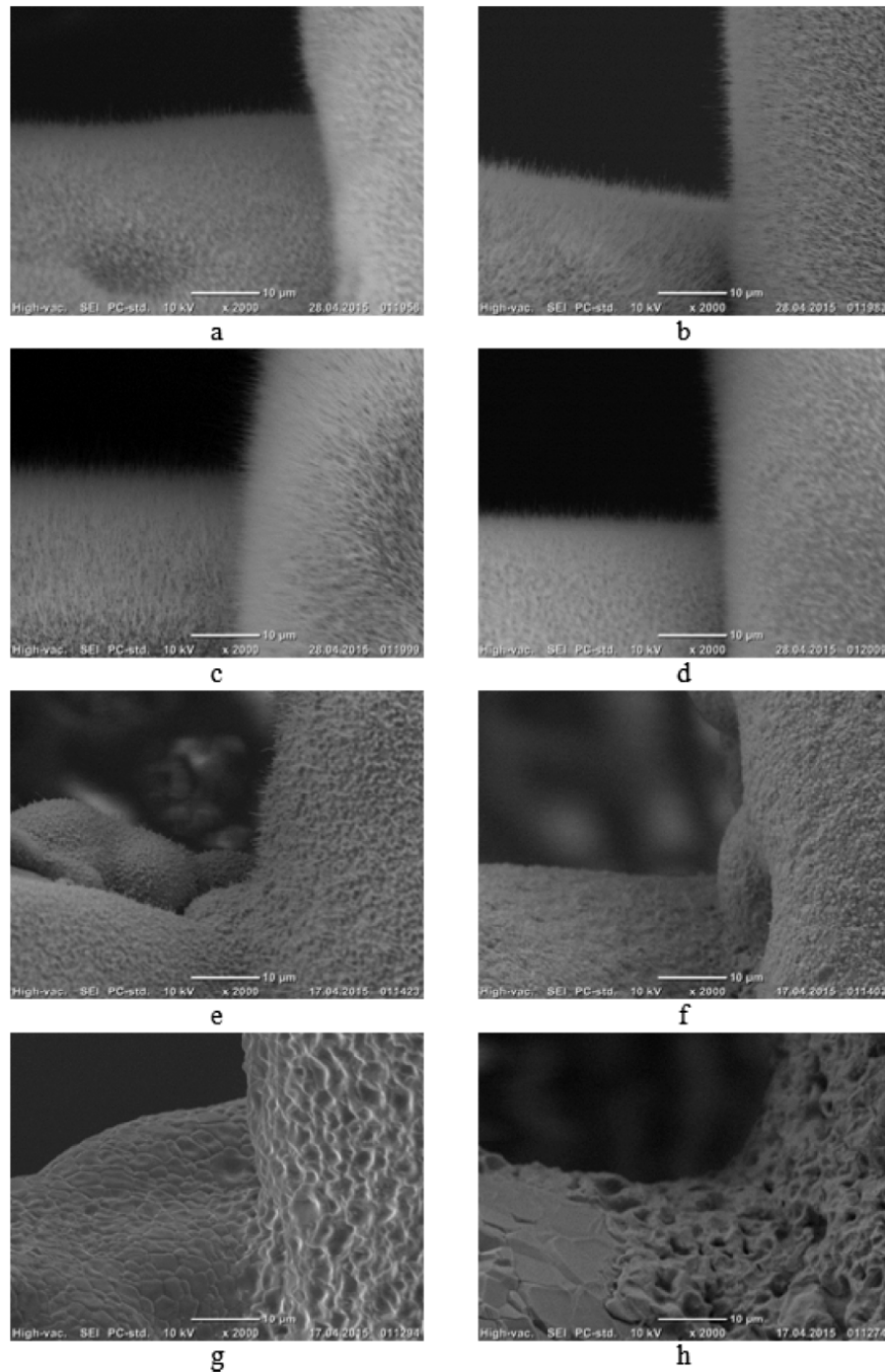


Fig. 8. SEM images of thermal study of copper oxide whisker structures: a – 200 °C, b – 300 °C, c – 400 °C, d – 500 °C, e – 600 °C, f – 700 °C, g – 800 °C, h – 900 °C (for 4 hours). Reprinted with permission from Ref. [45]; © 2017 Trans Tech Publications.

In the second case, whisker growth is due to chemical reactions, diffusion of atoms and their migration to the whisker surface. It should be noted that with this growth of the structure “from the top”, branchings can be formed (Fig. 6), which is *impossible* for the type of growth from the base [29].

Distinguishing the trajectories of the motion of atoms and the types of reactions that occur, two generalized growth mechanisms can be distinguished:

- vapor-liquid-solid (VLS);
- vapour-solid (VS).

The central role in VLS mechanism can be played by a “droplet” that has catalytic properties. As a droplet, a nanoparticle can also be used. There the whisker growth occurs at the droplet-whisker interface (Fig. 7).

The mechanism of the VS is similar to the VLS, except for the absence of a catalytic droplet. Adatoms that reach the top of the whisker due to diffusion are more

likely to be fixed on it due to energy advantage (the principle of minimizing free energy). For example, an axial screw dislocation in the whisker could serve as a nucleation centre for crystal growth, as indicated by Frank in 1952 [30].

3.3. Temperature and other environmental conditions

Metal whiskers. Arnold's article [31] contains historically the first data on the effect of temperature and the environment on the growth of Sn whiskers. The paper reviewed the experimental data, and discussed methods for preventing the growth of whiskers. In particular, it was noted that factors such as temperature, relative humidity, pressure, etc., affect the growth of whiskers only to some extent. Decrease in humidity and external temperature reduces, but does not suppress the growth of whiskers.

Further, Glazunova and Kudryavtsev [32] described in details the results of experiments on the growth of Sn whiskers on various substrates and in various external conditions, which allowed us to make several statements below.

1. The growth of whiskers on electrolytic tin coatings is a spontaneous process, independent of oxidation in a humid or dry atmosphere.
2. Temperature treatment at 100-180 °C for 1-24 hours showed a significant inhibitory effect on the growth of whiskers. This may be due to the relaxation of internal stresses at the base of the whisker. For example, heating of steel components with a tin coating on a copper substrate at 180 °C for 1 hour excluded the possibility of whisker growth even after 25 years of storage.

3. Electrodeposition at temperatures below 0 °C leads to a high growth rate of whiskers. This phenomenon explains the formation of a fine-grained structure of the base and the presence of significant internal stresses.

The effect of suppressing the growth of whiskers by thermal treatment was also investigated and confirmed in subsequent works [33-40]. On the other hand, cyclic heat treatment at low temperatures is capable (-55 °C to 85 °C) to accelerate the growth of whiskers [41-43]. There were studies also carried out on the effect of the electric field by applying the electric potential to the sample for the growth of whiskers. In Romm's work [44] a matte tin coating applied to the terminals of standard electronic components was subjected to an electrical voltage of 5 V. Subsequently, the samples were compared with coatings of the same series without the applied voltage. The authors conclude that the electric field can influence the growth mechanisms of whiskers, along with a multitude of other factors.

The studies on the growth of aluminum whiskers have shown an interesting feature [21]. Active growth of Al whiskers is observed only for a narrow temperature range between 200 and 240 °C, which again evidences the complex nature of the whisker formation process, which depends on the interplay of many factors.

Oxide whiskers. During the growth of CuO whiskers by annealing in the atmosphere, there is also an obvious dependence on the annealing temperature. Jiang [14] and Chen [21] studied the temperature dependence of the growth of CuO whiskers by heating copper foil. Temperatures in the range from 300 to 800 °C were tested, but whisker growth was detected only at temperatures of 400-700 °C. Kozlov et al. in Ref. [45] showed growth

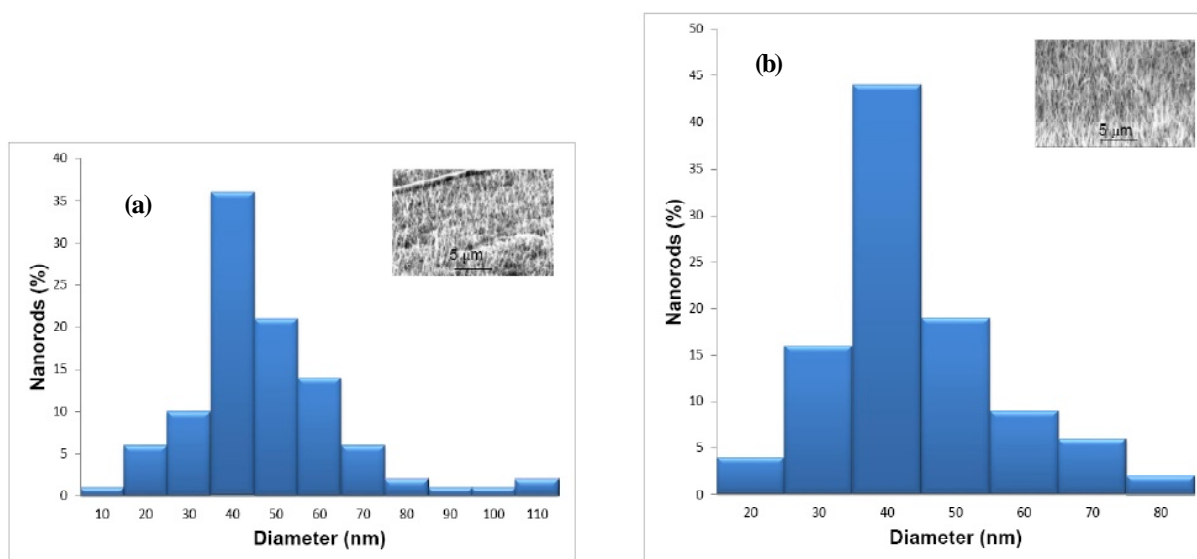


Fig. 9. The dispersion in the diameter of the nanorods prepared under an oxygen flow rate of 150 ml min⁻¹ and for annealing times of (a) 30 min and (b) 120 min at 400 °C. Adapted from Ref. [47].

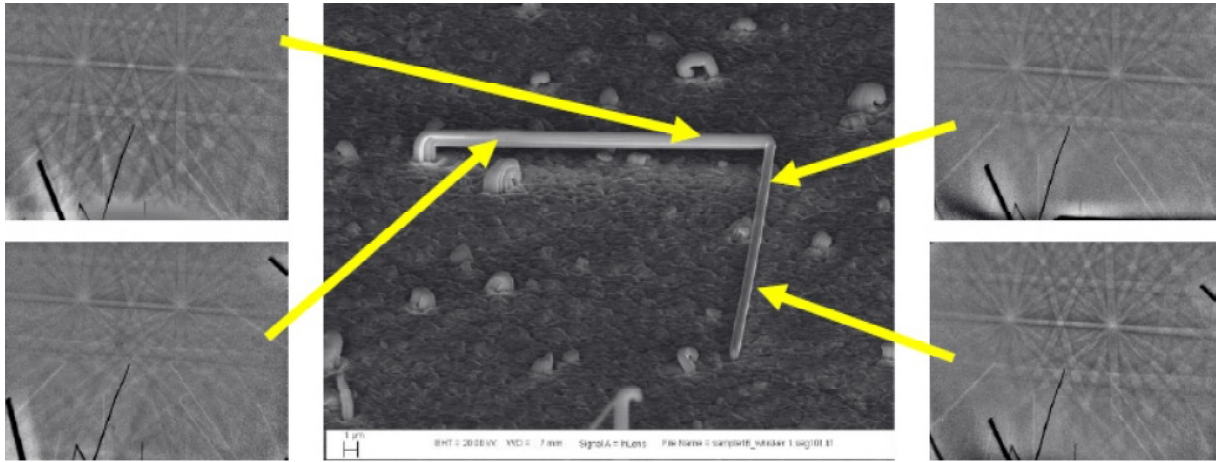


Fig. 10. Tin whiskers with “kinks”. Diffraction patterns indicate that the whisker itself is a single crystal, i.e. preserves crystallographic symmetry along its axis. Reprinted with permission from Ref. [50].

of CuO whiskers under heating copper on steel grid at temperature range from 200 to 700 °C (Fig. 8).

It should be noted that the cessation of whisker growth at temperatures above 700 °C was noticed earlier in [46], where this is explained by the acquisition of Cu₂O oxide at the base of the plastic properties layer and the subsequent *relaxation of mechanical stresses* in it.

Kumar gives in [47] a detailed account of the experiments on the growth of CuO whiskers, depending on various external parameters, including the annealing time, the annealing temperature, and the oxygen flow (Fig. 9). In particular, the paper notes the following points.

- The annealing time practically does not affect the average diameter of the whiskers.
- The period of “incubation” before the growth of the whisker serves to accumulate mechanical stresses. The time of “incubation” depends on the annealing temperature.
- Higher annealing temperatures result in larger whisker diameters.

As mentioned earlier, it is also possible to form CuO whiskers at room temperature and pressure in a chemical solution [26].

3.4. Internal structure of whiskers

Metal whiskers. Metallic whiskers are mostly monocrystalline structures, which was shown back in 1951 [2]. However, the direction of the whiskers may change as it grows. Such phenomena were called “kinking” and were first demonstrated in [48] for Sn whiskers. Subsequently, the kinks in the Cd and Zn as well as Sn whiskers were experimentally investigated [49]. It was concluded in [49] that between the whisker root and the base there is incoherent interface formed.

In detail, the kinks of tin whiskers were investigated at the Sandia National Laboratory (USA), as reflected in the report [50] (Fig. 10). The authors of the paper [50] concluded that there are two types of kinks. Type 1 kink does not lead to a change in the orientation of the grown segment, the morphology and the diameter of the whisker (Fig. 11).

Growth in this case often continues. On the contrary, a type 2 kink observed in the form of a bend leads to a change in the orientation of the whisker, morphology and diameter, which indicates the movement of the grain boundary inside the film. Such kinks often eliminate the conditions for the long-term growth of the whisker.

Oxide whiskers. A detailed characterization of CuO whiskers was carried out in [51]. It was shown that a typical structure for CuO whiskers is a single crystal with a twin boundary. Observations of the structure of the whisker point showed the presence of atomic steps, possibly serving to fix copper cations on the surface and playing an important role in the growth of whiskers.

In Ref. [52] nanowhisker (NW) cross-sections (Fig. 12) had been examined and it was shown that NW growth occurs along the $[1\bar{1}0]$ direction. It is the orientation inherent in all adjacent grains, as well as the direction belonging to the grain boundary (GB) planes such as $(11\bar{1})$, (001) , and $(11\bar{2})$. The $[1\bar{1}0]$ direction can be replaced with $[\bar{1}10]$, $[\bar{1}\bar{1}0]$, and $[110]$ because of the existing symmetry.

Another remarkable feature of CuO whiskers is the possibility of forming branched structures (Fig. 6). Such branched structures may be of interest for applications as a surface-developed material, for example for catalytic reactions [15].

In addition, branched structures in Ref. [52] with the following characteristics of CuO NW (see Fig. 13) were

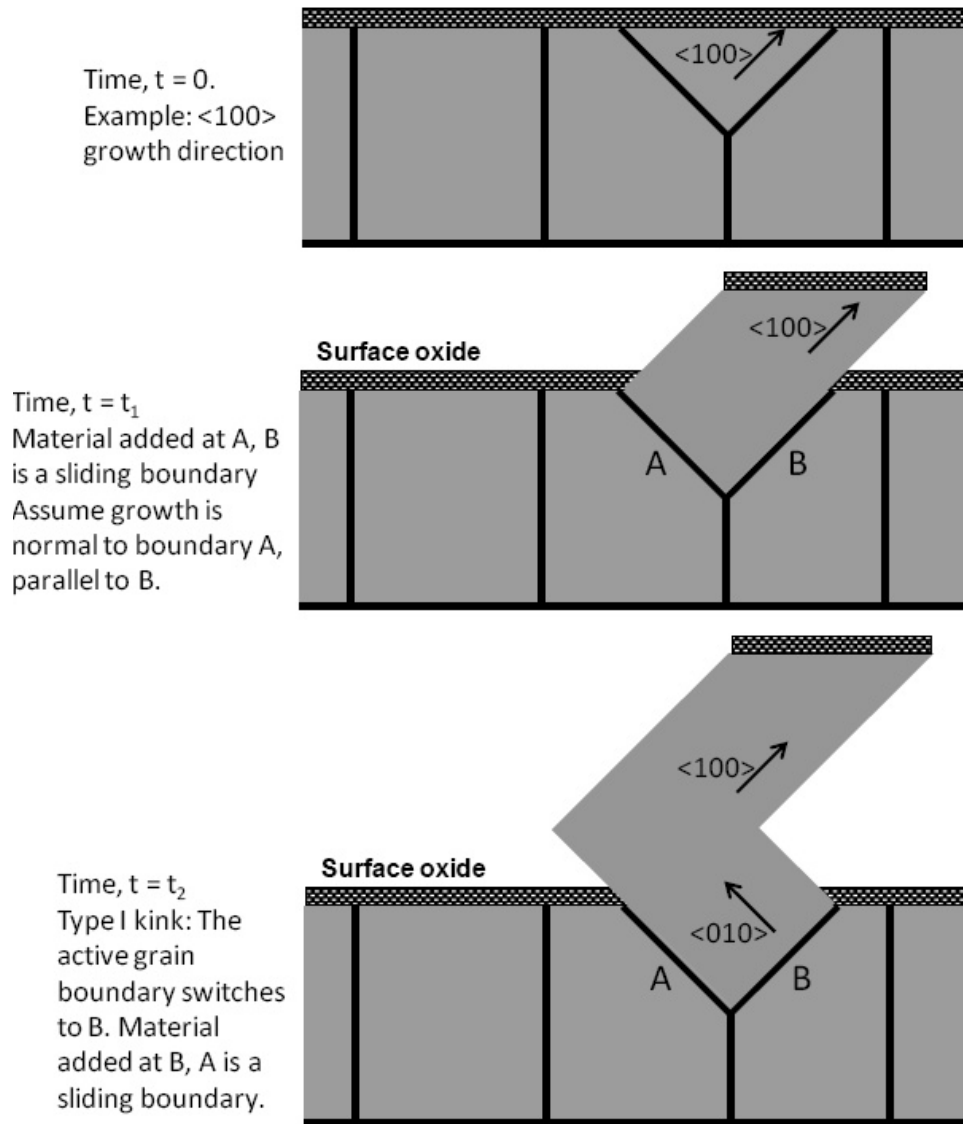


Fig. 11. Scheme of formation of fracture whisker type 1. Reprinted from Ref. [50].

distinguished: the top of the NWs appears in two types – flat and pointed. A closer view reveals that the top is formed by facets. In the process of growth, various defects are formed inside the NWs: regions along the growth direction with different orientations, twins, longitudinal defects along the growth line, kinks with a change in the growth direction, and globular formations.

3.5. Intrinsic structure of surface layer and substrate

Detailed studies of the influence of base and coating type on the growth of metal whiskers were carried out in [32]. Experiments were carried out on such bases as copper, nickel, zinc, brass, aluminium, silver, steel and tin. Tin coatings of various thicknesses were used, from very thin (less than 1 micron) to relatively thick (50 microns). It was shown that whiskers do not grow on very thin (micron) tin coatings, however, for thicker coatings,

a complex dependence on the thickness and type of the substrate was found. For copper bases, the density of whiskers and the rate of their growth were maximal at a thickness of 2-5 microns.

When a steel base was used, the density of whiskers and the speed are maximum at coating thicknesses between 5 and 10 microns. With brass bases, the growth of whiskers increased actively at thicknesses up to 20 microns. In addition, the duration of the incubation period differed on different grounds. All these observations speak in favour of the fact that the physics of processes inside the coating and on its boundary with the base is directly related to the growth mechanism of whiskers. The authors also [32] point out the following possible factors related to the role of coating and base. (1) Accelerated growth of tin whiskers on a brass base is due to the diffusion of zinc into the tin coating. The decrease in the rate of growth of the whisker with in-

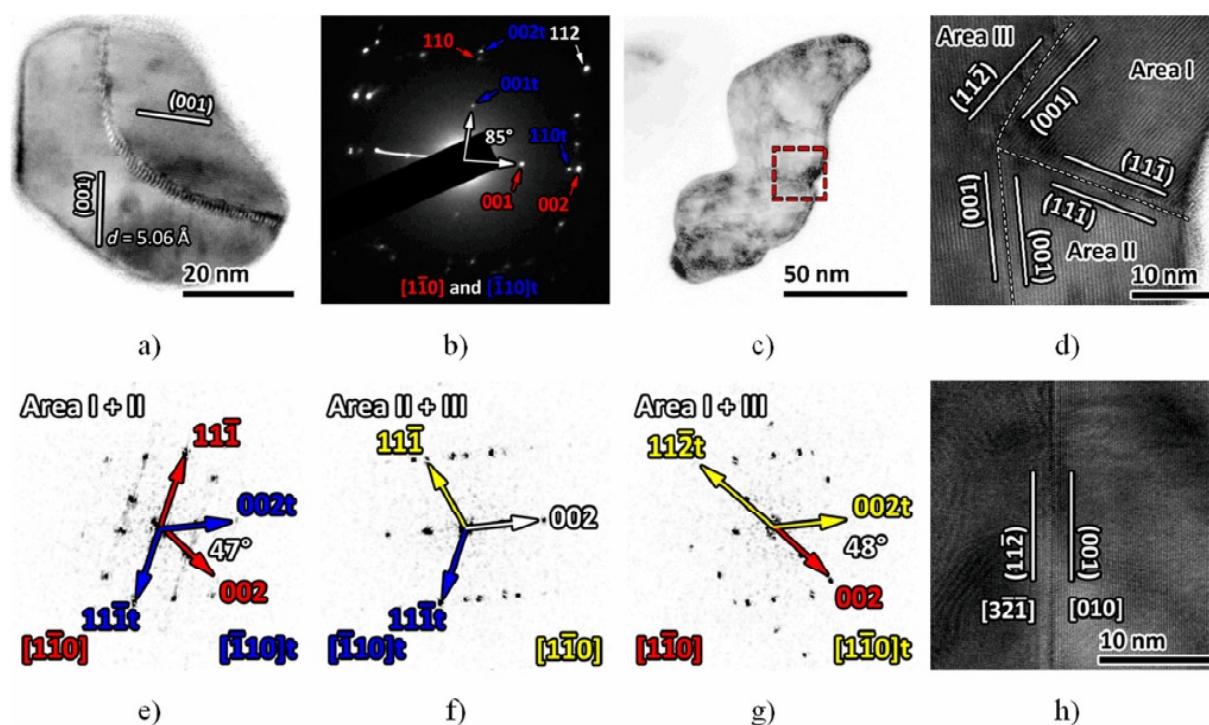


Fig. 12. HREM images of cross-sections of CuO nanowhiskers with: (a) bi-crystalline structure consisting of two crystals oriented along the $[110]$ and $[\bar{1}\bar{1}0]$ zone axes, respectively, and (c) poly-crystalline structure consisting of several crystals oriented along the $[1\bar{1}0]$ and $[\bar{1}\bar{1}0]$ axes; (b) SAED pattern of the one shown on 12a; (d) an enlarged image of the area, denoted by a dashed rectangle on 12c; (e, f, g) FFT patterns corresponding to the areas of grain boundaries (GBs) indicated in 12d; (h) HREM image of a GB between two crystals oriented along the $[3\bar{2}\bar{1}]$ and $[010]$ axes, respectively. Reprinted from Ref. [52] by permission of the publisher (Taylor & Francis Ltd, <http://www.tandfonline.com>).

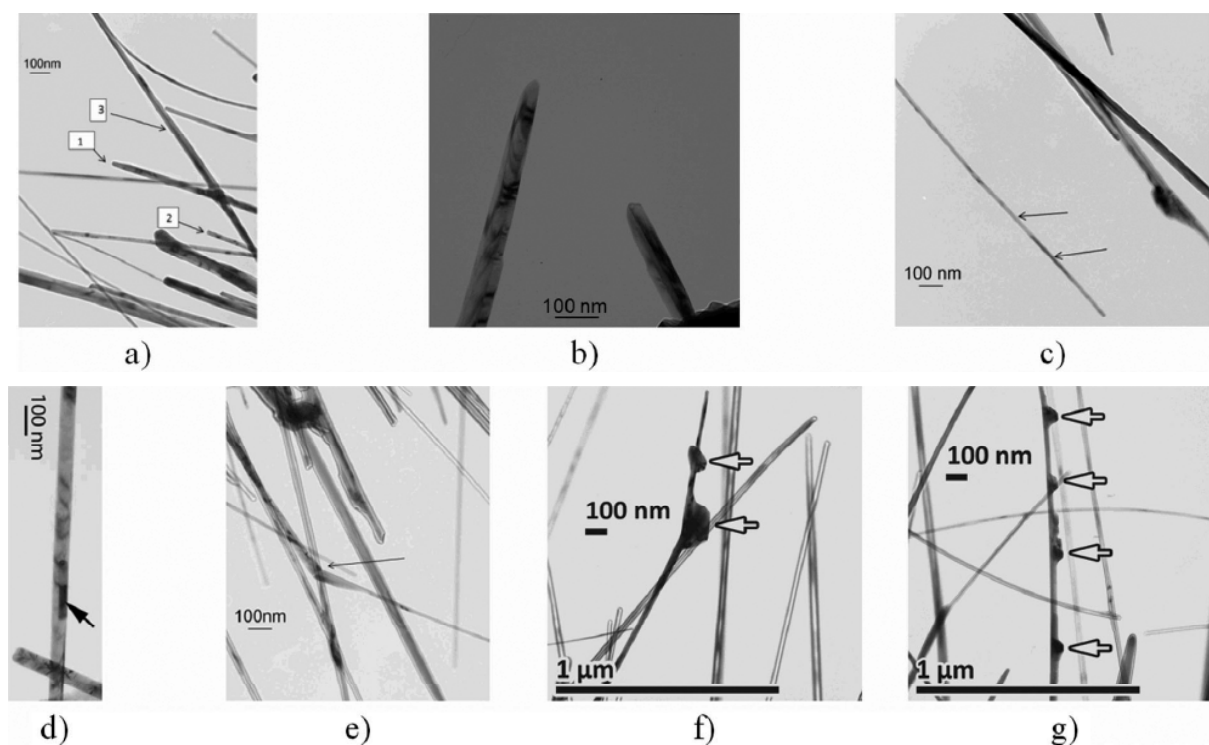


Fig. 13. Structure and morphology of CuO nanowhiskers (NWs): (a) different shapes (1, 2) of the NW top and longitudinal defect in the NW (3); (b) faceting of the NWs; (c) arrows point at areas of an NW with different orientation; (d) twins; (e) kinks; (f, g) globular formations. Reprinted from Ref. [52] by permission of the publisher (Taylor & Francis Ltd, <http://www.tandfonline.com>).

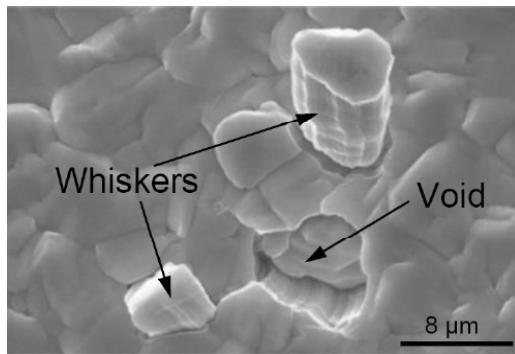


Fig. 14. SEM image of the tin coating. The emergence of voids with the growth of a tin whisker. Adapted from Ref. [54].

creasing thickness of the coating is probably associated with a decrease in internal stresses in it.

(2) The high growth rate of tin whiskers on coatings applied at low temperatures is explained by the large number of defects and internal stresses.

(3) These factors suggest that incubation and subsequent growth of tin whiskers is a special type of recrystallization of the tin coating.

It is necessary to note such a phenomenon, observed in tin coatings, as the formation of voids (cavities). In [53] the flow mechanisms for the growth of tin whiskers on steel substrates by using coatings of various thicknesses and applying mechanical pressure were experimentally investigated. For a certain set of sample parameters, void formation was observed instead of whisker growth. The authors explain the lack of whiskers by too thick coating and / or too low pressure.

Moreover, it is possible for a whisker to form together with voids at a close or even an adjacent distance, as indicated by Galyon [54] (Fig. 14). This behavior evidences the possibility of non-trivial mechanisms of material transfer with the growth of the whisker.

Protection layer. As it is known, the surface of many metals has the property of oxidizing in air, forming an oxide layer. The role of such an oxide layer for the growth of whiskers is still not fully understood. In some works such an interlayer is called “protective”. As will be shown below, it is claimed that it can inhibit the relaxation of internal stresses up to point of crack formation in it and the growth of the whisker through it.

Barsoum, investigating the growth of indium whiskers (In) in Zr₂InC samples in his work [55] suggested that the driving force for whisker growth is the reaction between oxygen and the metal sprouting through the interlayer. As a result, the expansion of the volume creates compressive stresses that push the whisker outward. However, this hypothesis cannot explain the influence of the thickness of the coating on the growth of whiskers.

It is interesting to note that a similar phenomenon accompanies the growth of silver whiskers (Fig. 15), as described in the work of Chudnovski [20]. Since silver is relatively slightly susceptible to oxidation, the role of oxygen in the case of silver can play sulphur. Thus, the “protective” layer will be silver sulphide, which was shown in [20]. It is important to note the fact that the whiskers themselves consist of pure silver and do not contain sulphur, and the sulphide is found only on the surface.

Structure of the surface layer and base boundary. The metallic tin coating undergoes structural changes during the whisker incubation period, as shown in Egli’s studies [56]. Egli observed the internal structure of the tin coatings over time by etching. It was found that there is an active movement of defects and changes in the internal structure of the coating. In particular, after etching around each of the whiskers, grooves were observed (see Fig. 16), which may indicate the presence of a new crystalline structure of the coating near the whisker. The author also hypothesizes that the special orientation of the faces at a small angle contributes to the relaxation of internal stresses through the ejection of the whisker.

Galyon in [57] had been investigating the tin coating on a copper base, showed the structure of the boundary of their in a cross-sectionally (Fig. 17). The presence

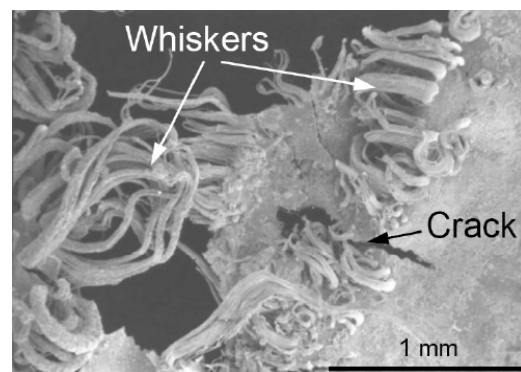


Fig. 15. SEM image of silver whiskers. Adapted from Ref. [20].

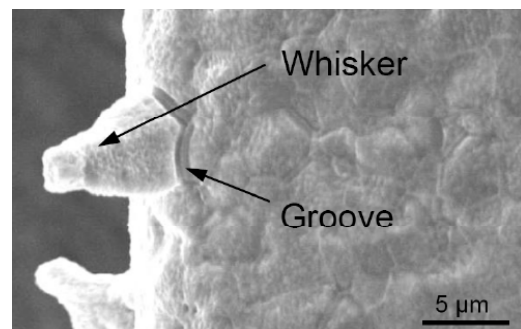


Fig. 16. SEM image of the tin coating after etching, whisker and grooves around it. Adapted from Ref. [56].

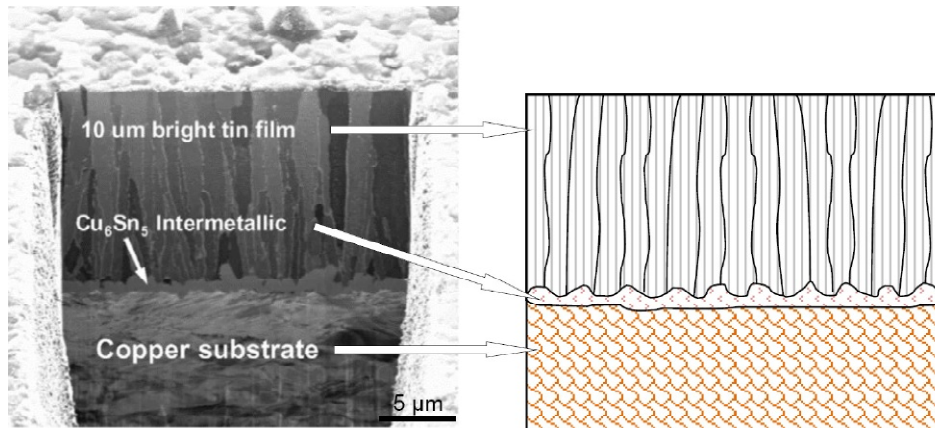


Fig. 17. Microstructure of tin layers on a copper base, Cu_6Sn_5 intermetallic in the interface between them. Adapted from Ref. [57].

of an intermetallic Cu_6Sn_5 compound at the interface was shown. The work indicates that the formation of such an intermetallic compound after coating can lead to *internal mechanical stresses*, which will serve as a driving force for the growth of whiskers.

When copper (copper foil) is annealed, a multilayer structure is also formed, consisting of the initial copper, Cu_2O oxide and CuO oxide. Work [51] demonstrated studies of the evolution of oxide layers during annealing (Fig. 18). The author assumes that phase transformations at the interfaces between oxides can be a source of *internal mechanical stresses* for the growth of the CuO whisker. This allows us to make a bridge between the possible growth mechanism of metal and oxide whiskers: in both cases the formation of a layered structure would lead to *internal mechanical stresses*.

3.6. Internal mechanical stress in the surface layer and substrate

Metal whiskers. From the very beginning of whisker research, there was a commonly posted hypothesis that the presence of internal mechanical stresses is one of the basic necessary conditions for whisker growth. In the work of Shibutani et al. [58] experiments were carried out to test the influence of stresses and material creep on the growth of whiskers by applying pressure on the coating with special sharp needles (Fig. 19).

Oxide whiskers. The influence of internal stresses on the growth of CuO whiskers was shown in [24], where the authors describe the method of manufacturing copper microcontainers. The growth of whiskers occurs during annealing for 3 hours at a temperature of 400°C on the inner sides of the container. The authors attribute this phenomenon to the presence of compressive stresses on the inner sides, which serves as a driving force for the growth of whiskers.

4. THEORETICAL MODELS AND INTERPRETATIONS OF WHISKER GROWTH

4.1. Dislocation models of whisker growth

Peach's model. Historically, the first proposed model for the growth of metal whiskers was Peach's model

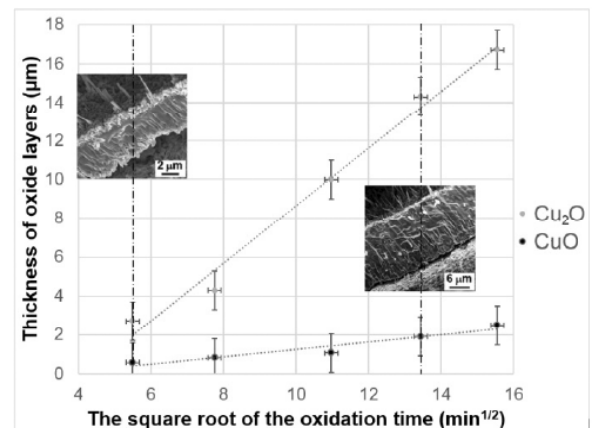


Fig. 18. The thickness of oxide layers as a function of time during oxidation. Adapted from Ref. [51].

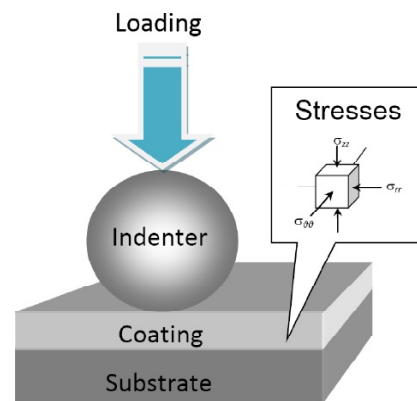


Fig. 19. Schematic illustration of the initiation of growth whisker by contact load. Adapted from Ref. [58].

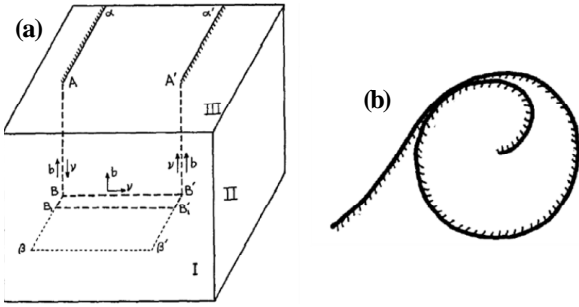


Fig. 20. Peach's whisker growth model. Reprinted from Ref. [59], with the permission of AIP Publishing.

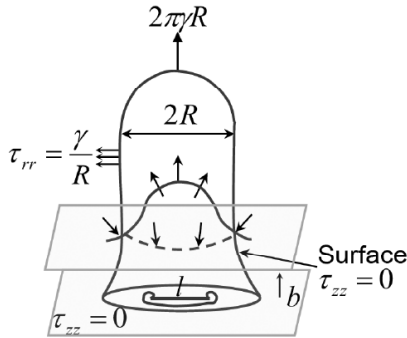


Fig. 21. Eshelby's model of whisker growth. Adapted from Ref. [8].

[59]. It suggested using dislocations as a structural basis for the motion of atoms in the formation of the whisker (Fig. 20). Despite the fact that this model is of theoretical interest, it did not find an experimental confirmation. Further experimental studies have pointed to another type of whisker growth in the case of metal whiskers.

Eshelby's model. Eshelby's model [8] was the next theoretical model recalling dislocations (Fig. 21). It was based on the emergence of a prismatic dislocation loop in the Frank-Read source and its further vertical slip along the whisker axis under the influence of fields of mechanical stresses. The output of such a prismatic dislocation loop to the surface means an increase in the length of the whisker by an amount equal to the value of the Burgers vector of the dislocation loop.

In connection with Eshelby's model, it should be noted that in spite of the fact that the mechanism of nucleation of a prismatic dislocation loop was not defined, the mechanism of nucleation of loops in crystals from a helicoidal dislocation was later experimentally shown in [60].

Lindborg's model. A new dislocation model of the growth of metal whiskers was proposed in [9], which has much in common with Eshelby's model. It also distinguishes 2 stages: (1) nucleation and expansion of dislocation loops; (2) their subsequent exit to the whisker surface (Fig. 22). The mechanism of diffusion of vacancies necessary for the expansion of dislocation loops is also considered in this paper. It is concluded that the rate of development of the first stage is determined by distant diffusion and physical conditions are proposed that control the rate of growth of the whisker.

Model of whisker growth in small particles. The formation of whiskers in metallic small particles has attracted the attention of researchers rather recently [22]. A dislocation model for the growth of whiskers in small pentagonal particles was proposed [10,11]. It shows that whisker growth can be one of the mechanisms of relaxation of internal mechanical stresses inherent in pentagonal crystals. Calculations of the energy balance are presented for the splitting of two dislocation loops of the opposite sign (Fig. 23). One of the loops, reaching the surface of the particle, lengthens the whisker (similar to the models of Eshelby and Lindborg).

4.2. Models of structural transformations in the substrate

Following the hypothesis that internal mechanical stresses are the driving force for the growth of whiskers, several works have been devoted to modelling of the evolution of internal stresses in metal coatings. The simulation of the density of elastic energy was carried out in [61] on the basis of data from experimental samples of tin coatings. Experimentally measured crystallographic orientations of the grain facets by the

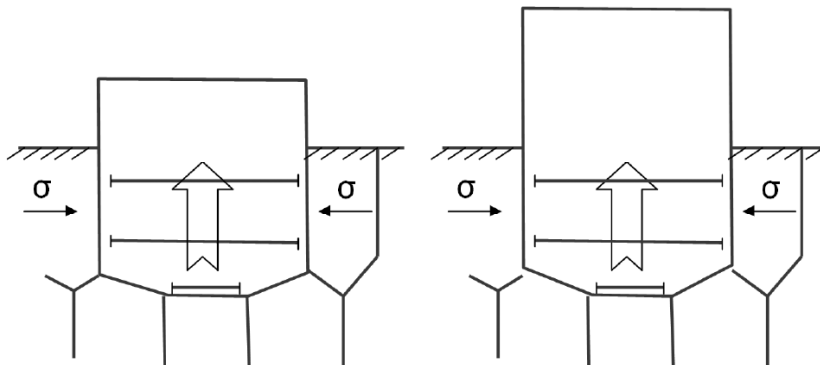


Fig. 22. Lindborg's model of whisker growth. Adapted from Ref. [9].

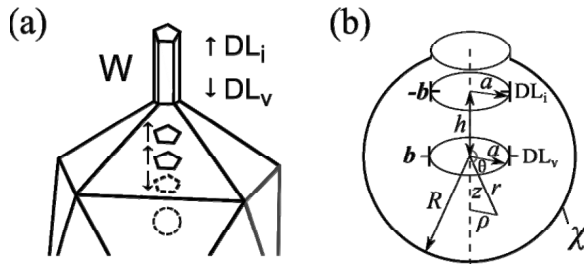


Fig. 23. The growth of the whisker from the pentagonal particle. Physical model of the growth of a whisker crystal from an icosahedral particle with an internal cavity by means of dislocation prismatic loops (a). The nucleation and separation of prismatic dislocation loops in an icosahedral particle. Geometry of the computational model (b). Reprinted from Ref. [11] with permission; Copyright © 2014, Springer Nature.

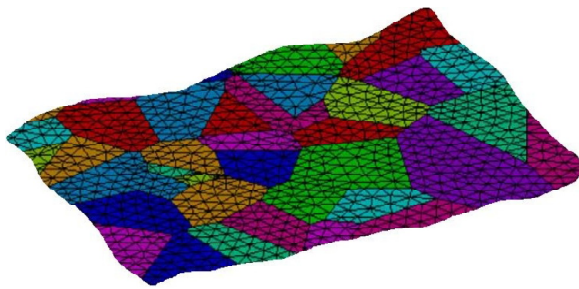


Fig. 24. Typical grid for finite element calculations with boundary conditions. Tin grains with different orientations are marked with different colors. The copper base is modeled as an isotropic material. Adapted from Ref. [61].

X-ray diffraction method were taken and incorporated into the design model of the coating structure on the basis of the finite element method (Fig. 24).

Further, in the numerical model, a cyclic thermal treatment was carried out and a map of the density of elastic stresses was constructed. The obtained map is com-

pared with observations of whisker growth on the experimental sample and a conclusion is made about the presence of a direct correlation between the simulated mechanical stresses and the conditions for the growth of the whisker.

In a more recent paper by Buchovetsky et al. [62] an attempt was made to model the mechanical stresses in a tin coating on a copper base by the finite element method. The formation of the intermetallic Cu_6Sn_5 serves as a stress source in the model (see Fig. 25).

Simulation of stress distribution during the annealing of copper samples due to uneven thermal expansion was also considered in [21] (Fig. 26). Comparison of the experimental samples with the stress map confirmed the expected correlation between the growth of whiskers and the presence of stresses.

4.3. Diffusion model of growth

Metal whiskers. A model for the growth of tin whiskers based on a diffusion mechanism was proposed by Tu et al., see, for example, [12]. The model assumes a diffusion flux at grain boundaries under the influence of a special distribution of internal pressure. In the same paper, a model is proposed in which material transfer occurs due to the “liquid flow” at the grain boundaries. In both cases of occurrence of internal stresses is explained by the formation of the intermetallide Cu_6Sn_5 , the oxide film, the generation and absorption of vacancies (Fig. 27). Thus, in the places of rupture of the oxide film, conditions are made for the diffusion or flow mechanisms of the growth.

An alternative concept for the growth of whiskers Sn was proposed by Smetana in [4]. It is based on the following assumptions (see the illustration in Fig. 28).

1. The driving force for the growth of the tin whisker is the compressive stresses in the tin coating.

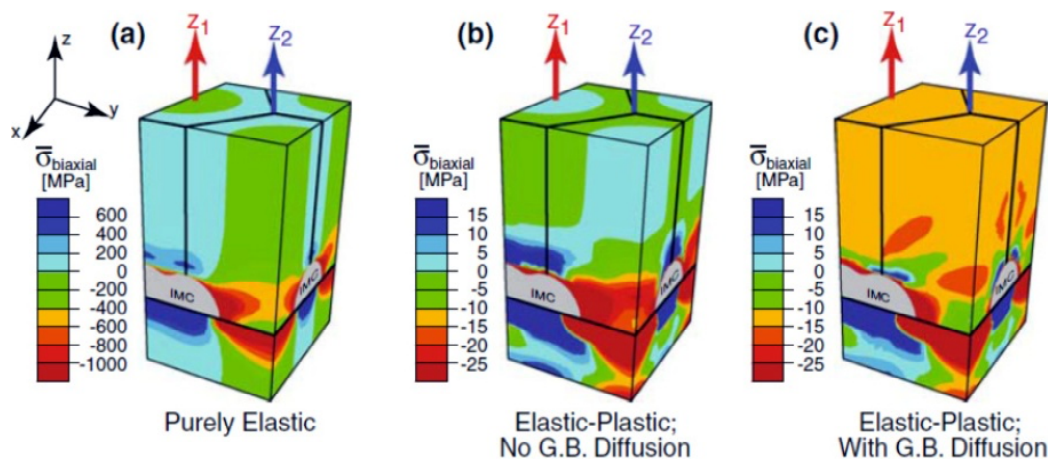


Fig. 25. Stress distribution in the tin coating on copper with intermetallic interlayer in the finite element model. Reprinted from Ref. [62], under an open access license.

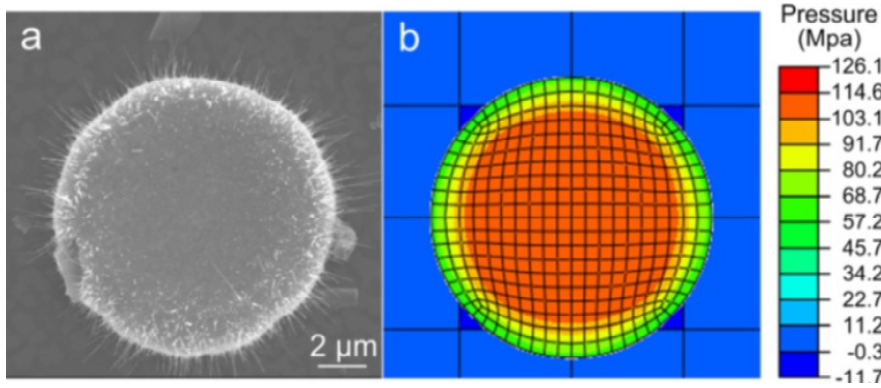


Fig. 26. (a) CuO whiskers on a copper disk located on a flint base. (b) Distribution of stresses in a copper disk on the surface during annealing. Reprinted from Ref. [21], with the permission of AIP Publishing.

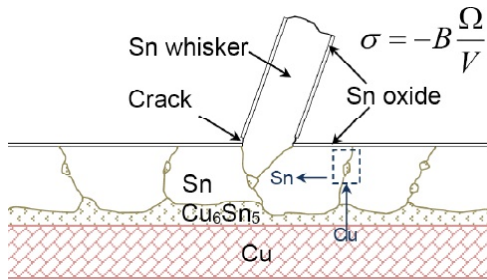


Fig. 27. Whisker growth diffusion model by Tu et al. Adapted from Ref. [12].

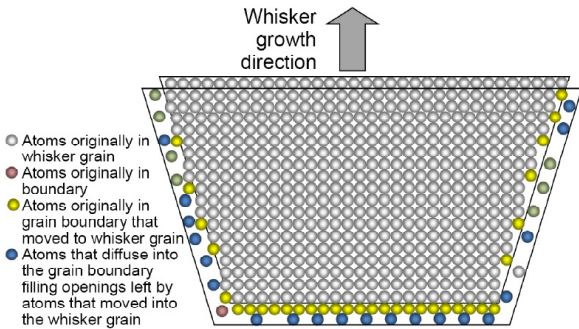


Fig. 28. Tin whisker growth model proposed by Smetana. Adapted from Ref. [4].

2. The inclined grain boundaries distinguish the growth grains of whiskers from others. The author of the model is inclined to assert that such an orientation of grain boundaries is in general a result of recrystallization.
3. The inclined grain boundaries lead to a lower stress in the whisker growth grains relative to the vertical grain boundaries. This is the source of the stress gradient, which leads to the diffusion of tin atoms to the base of the whisker.
4. Compressive stresses on the inclined grain boundaries lead to creep and whisker growth.
5. This process will continue as long as the compressive stresses and the mobility in grain boundaries persist.
6. The oxide film can serve as another source of compressive stresses, and also can increase the diffusion rate Sn at the grain boundaries. It also leads to an

additional effect of shear deformation on the whisker grain. High humidity can enhance this effect due to the difference in the molar volume of hydrogenated tin oxide compared to unhydrogenated.

Galyon’s model of whisker growth proposed in Ref. [54] was intended to explain the phenomenon of the transfer of tin whisker material and the formation of voids (Fig. 29). The model considers the diffusion motion of vacancies and Sn atoms under the influence of given mechanical stresses in the granular structure of the Sn coating.

In [53] Howard attempted to explain the high growth rates of tin whiskers. The author claims that the speed

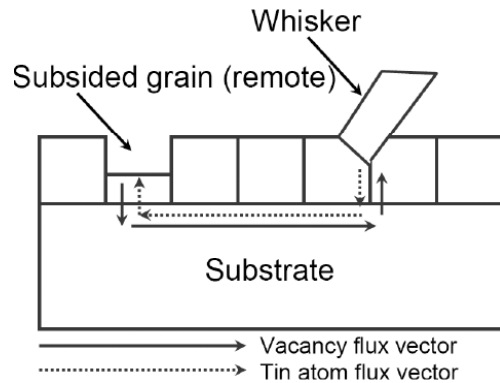


Fig. 29. Tin whisker growth model proposed by Galyon. Adapted from Ref. [54].

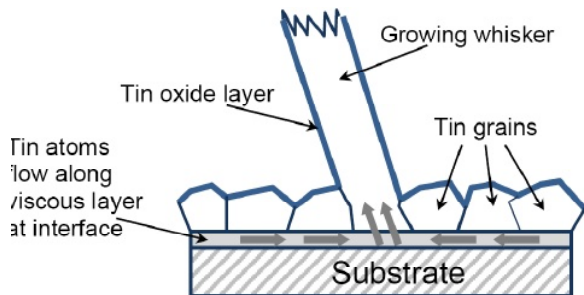


Fig. 30. Tin whisker growth model proposed by Howard et al. Adapted from Ref. [53].

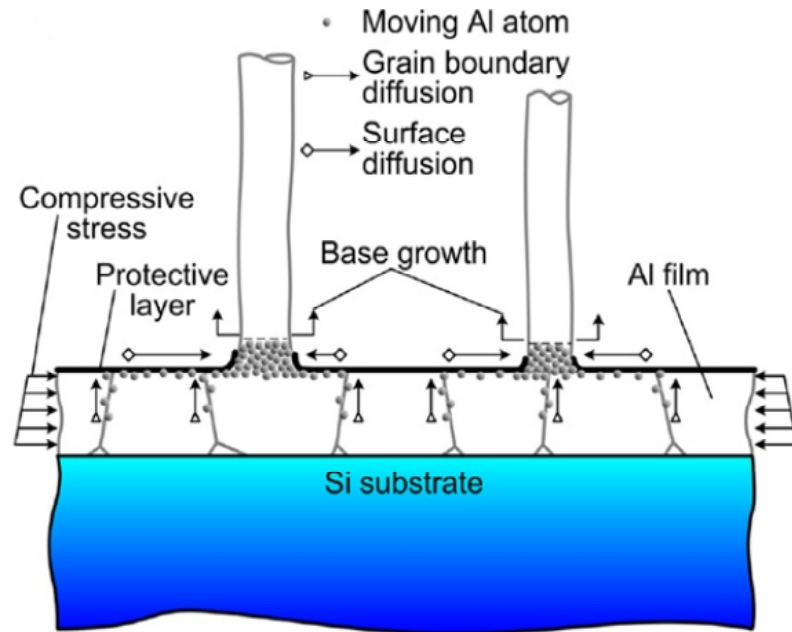


Fig. 31. Aluminium whisker growth model proposed by Chen et al. Reprinted from Ref. [21], with the permission of AIP Publishing.

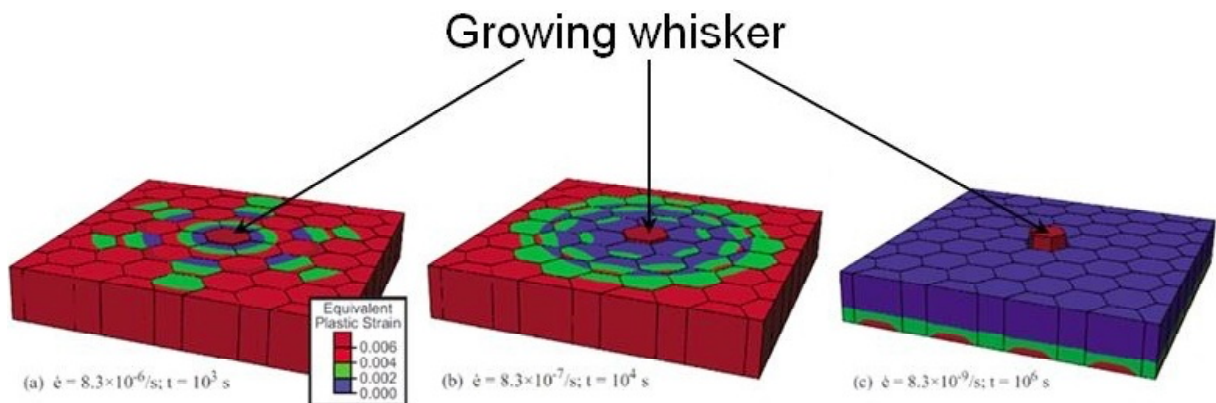


Fig. 32. Finite element modelling of tin whisker growth by Buchovetsky et al. (a, b, c) Structure and maps of plastic deformation at various parameters of the model. Adapted from Ref. [63].

of ordinary diffusion in a metal is not sufficient to ensure the observed rates of growth of whiskers, and suggests considering the mechanism of the viscous flow of tin atoms at the coating-base interface (Fig. 30).

Paper [21] contains a diffusion model of growth of aluminium whiskers (Fig. 31). It generally agrees with other diffusion models of tin whiskers. It indicates the role of a protective film, compressive stresses, and diffusion of atoms along the grain boundary.

It should be noted separately the growth model of the tin whisker, based on the finite element method [63] (Fig. 32). The calculations are based on the continuum solid model with plastic deformation and diffusion at grain boundaries, under the conditions of intermetallide formation. A simple analytical model is also presented for estimating the rate of growth of the whisker and is found to be in agreement with the experimental measurements.

Oxide whiskers. The concept of growth of CuO whiskers as a result of annealing copper samples is presented in paper [21] (Fig. 33). It considers the diffusion of Cu atoms along the grain boundaries and further surface diffusion on the whisker. The driving force for diffusion along the grain boundaries is mechanical stresses in the oxide film, and for surface diffusion, the gradient of Cu ion concentration and the local stress gradient at the microscopic level.

The model for the growth of the whisker CuO was also proposed by Yuang [51]. For the most part, it agrees with the model of Chen's et al., but in addition it provides an explanation for the presence of a twin boundary in CuO whiskers. The author of the model assumes that the twin boundary is a consequence of the origin of the whisker in places with a special arrangement and orientation of the surface facets of the oxide. The paper also gives an extensive discussion of the possible chemi-

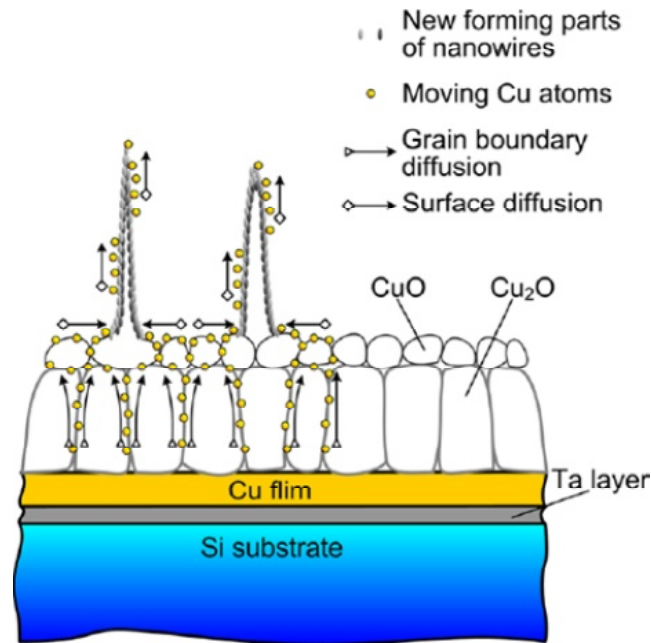


Fig. 33. The diffusion model of CuO whisker growth proposed by Chen et al. Reprinted from Ref. [21] with the permission of AIP Publishing.

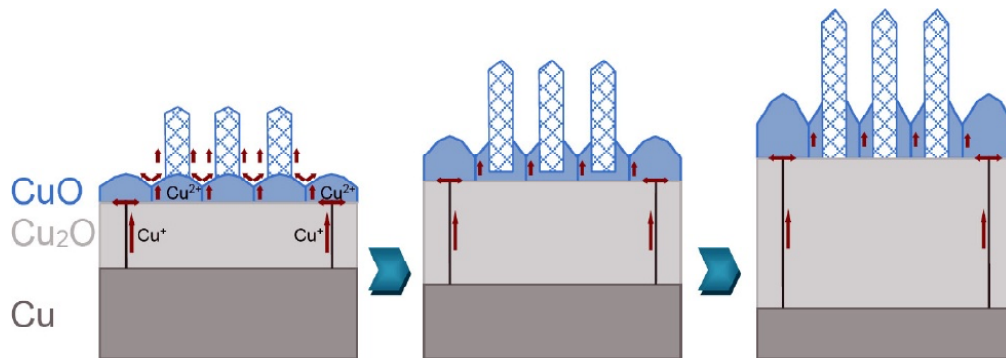


Fig. 34. Diffusion model for CuO whisker growth by Yuan et al. Structural change in the interlayer of oxide and elongation of the root of the CuO whisker with time. Adapted from Ref. [51].

cal and physicochemical aspects associated with the diffusion motion of atoms with the growth of the whisker. In conclusion, the article presents experimental data and explanations of structural changes in the base (“root”) of the whisker, namely, the extension of the whisker deep into the coating (Fig. 34).

5. Recent research on whiskers and cavities in small particles

In this section let us take a brief review on the complex cases where structural transformations in micro- and nanoparticles are induced by a chemical reaction leading to formation of internal cavities (voids) and nanowhiskers or other kinds of developed surface.

A simple hydrothermal method for fabricating nanocubes of single-crystal metal oxide and polycrystalline metal with an internal cavity was devel-

oped in [64] (Fig. 35). Chemical processes can be represented in two steps: Cu^{2+} ions are converted to the oxide phases of CuO and Cu_2O , and then to metallic copper Cu in a reducing medium. Instead of forming polycrystalline Cu_2O nanospheres, in particular, nanocrystalline CuO particles can aggregate into porous Cu_2O nanocubes with a well-defined cubic structure, where Cu_2O crystallites are attached to each other, preserving the overall cubic symmetry (Fig. 36).

Due to the presence of space between the crystallites in the Cu_2O aggregates, pore coarsening and the formation of nanocubes with a central cavity can be carried out. The authors point to Ostwald’s mechanism as playing a key role in this process of evacuation of the solid phase.

The method for preparing CuO microspheres with a developed surface was described in [65]. There, a thermal chemical process at 100 °C and a duration of 12

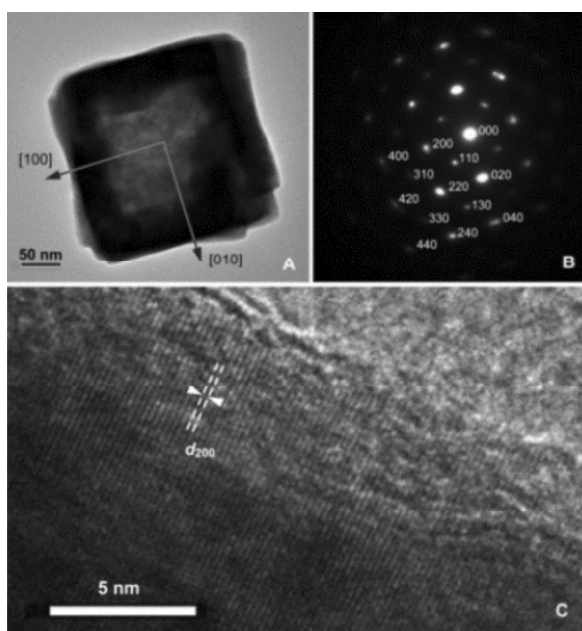


Fig. 35. (A and B) TEM image of a hollow cubic Cu_2O particle and its diffraction pattern. (C) High-resolution TEM image of a cubic particle Cu_2O . Reprinted with permission from Ref. [64]; Copyright 2006 American Chemical Society.

hours with CuCl_2 and KOH as initial materials was proposed. Many parameters, such as the volume fraction of water with respect to ethylene glycol, the amount of KOH , and the reaction temperature, can influence the phase composition and morphology of the final product.

A high proportion of water with respect to ethylene glycol and the amount of KOH , at low temperatures, led to the formation of hedgehog-shaped CuO microspheres. The authors indicated that such microstructures have good photocatalytic properties for the degradation of some organic paints, which has potential applications in wastewater treatment and environmental protection.

The similar hedgehog-shaped copper oxide microspheres with superb photocatalytic properties were obtained by simple method annealing of icosahedral small copper particles in Refs. [45,66]. Heating to 400-500 °C and holding at these temperatures for 2-5 hours lead to the mass formation of nanowhiskers with diameter 40-100 nm, length of 10-20 microns, and a surface density of 10^8 - 10^9 cm^{-2} on the surface of an icosahedral particle (Fig. 37).

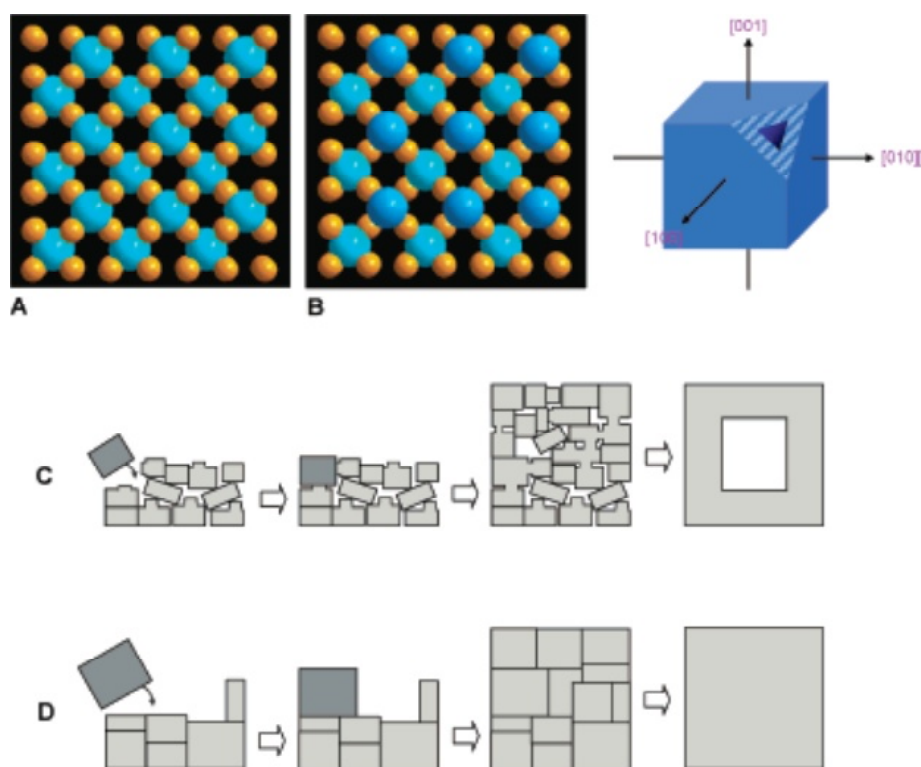


Fig. 36. Models of the Cu_2O surface of crystalline planes (100): (A) the plane completed by the Cu cation (Cu atoms are shown in orange), and (B) the plane completed by the O_2^- (O_2^- anions are shown in blue and dark blue). Reducing the formation of cubic structures under different experimental conditions: (C) with less water, the Cu_2O crystallites are smaller and the Cu_2O (100) surfaces are more rough, resulting in large discrepancies between crystallites and a lower packing density when the central cavity is formed by the Ostwald mechanism, and (D) with a larger water content, the Cu_2O crystallites are larger and the Cu_2O (100) surface is smoother, leading to a better mix of crystallites and a higher packing density. Crystallites CuO , attached to cubes Cu_2O (shown in gray) are represented by dark gray rectangular blocks. Reprinted with permission from Ref. [64]; Copyright 2006 American Chemical Society.

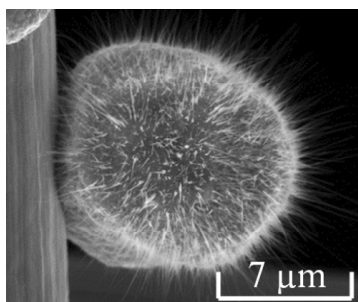


Fig. 37. SEM images of hedgehog-shaped copper oxide microsphere with a developed surface. Reprinted from Ref. [66], with permission © (2014) Trans Tech Publications.

It was shown in [67] that the growth of nanowhiskers on copper particles has a size effect (Fig. 38). At a particle size of about 3 micrometers or below, the growth of nanowhiskers was not detected, and at 10 micrometers or more, the particles were covered with straight and unbranched whiskers perpendicular to the surface. Thermogravimetric analysis and X-ray diffraction were

used to study this size effect and the evolution of different phases of copper and copper oxide over time. The authors also had found that these particles become hollow after oxidation and proposed a mechanism based on the Kirkendall effect.

A simple two-step method for synthesizing CuO hollow nanospheres on porous Si nanowires is proposed in [68] (Figs. 39 and 40) using a reduction reaction and subsequent calcination. In the process of calcination, Cu nanoparticles were not only oxidized to CuO, but also initially solid nanoparticles were transformed into hollow ones due to the Kirkendall effect. The resulting spheres of CuO in the majority have a diameter of about 30 nm and are evenly distributed on porous nanowires without aggregation. Electrochemical tests have shown that such hybrid nanostructures are highly susceptible to electro-oxidation to hydrazine, which can find applications in electrochemical sensors.

In [69] spherical CuO particles with a hierarchical architecture and pores were fabricated using a simple single-vessel template-free method (Figs. 41 and 42).

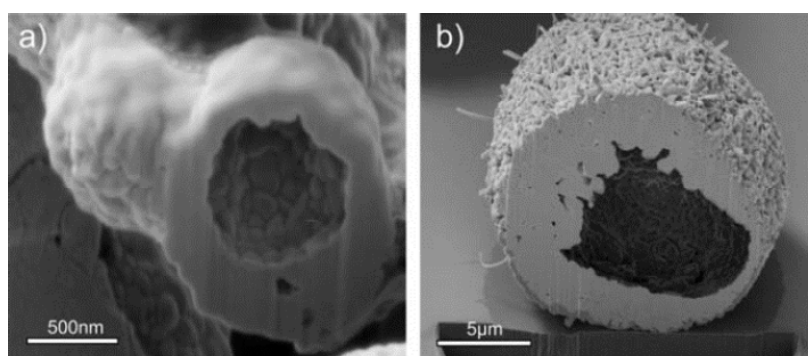


Fig. 38. SEM images of particles of copper oxide, cut by an ion beam. Cavities could arise under the influence of the Kirkendall effect and the diffusion of copper from the center outwards. Used with permission of Royal Society of Chemistry, from Ref. [67]; permission conveyed through Copyright Clearance Center, Inc.

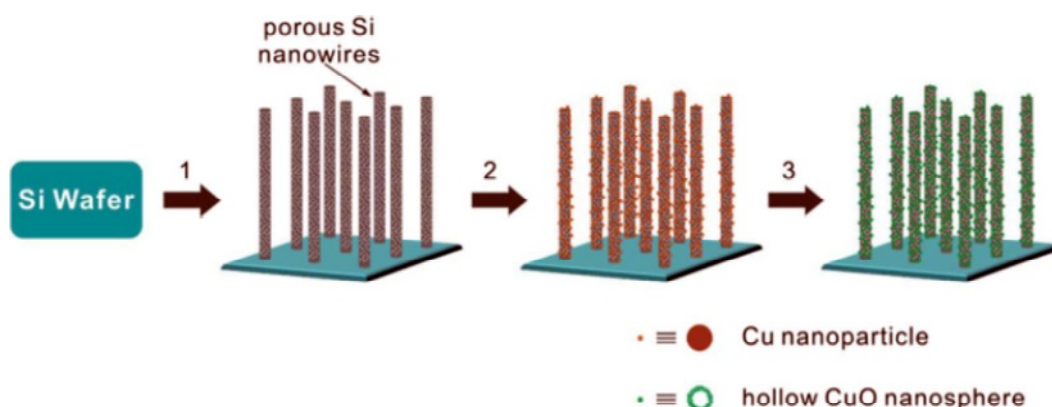


Fig. 39. The synthesis of CuO hollow nanospheres uniformly distributed over porous Si nanowires: (1) preparation of porous Si nanowires through the etching of a strongly doped silicon substrate, supported by silver; (2) Cu²⁺ reduction on the surface of manufactured nanowires, and (3) hollow CuO nanospheres after calcination of Cu particles in air. Used with permission of Royal Society of Chemistry, from Ref. [68]; permission conveyed through Copyright Clearance Center, Inc.

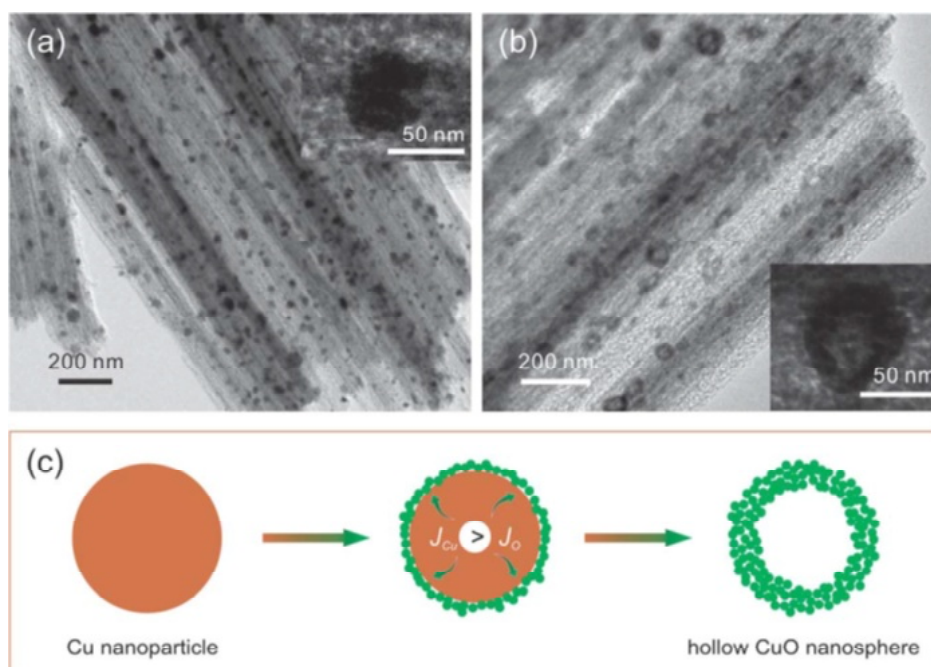


Fig. 40. (a) TEM images of copper nanoparticles, uniformly distributed on porous Si nanowires, on the inset shows a separate Cu nanoparticle. (b) TEM image of hollow CuO nanospheres on porous Si nanowires, the inset shows individual hollow CuO nanospheres. (c) mechanism for the conversion of Cu nanoparticles into hollow nanoscale CuO during calcination in air. Used with permission of Royal Society of Chemistry, from Ref. [68]; permission conveyed through Copyright Clearance Center, Inc.

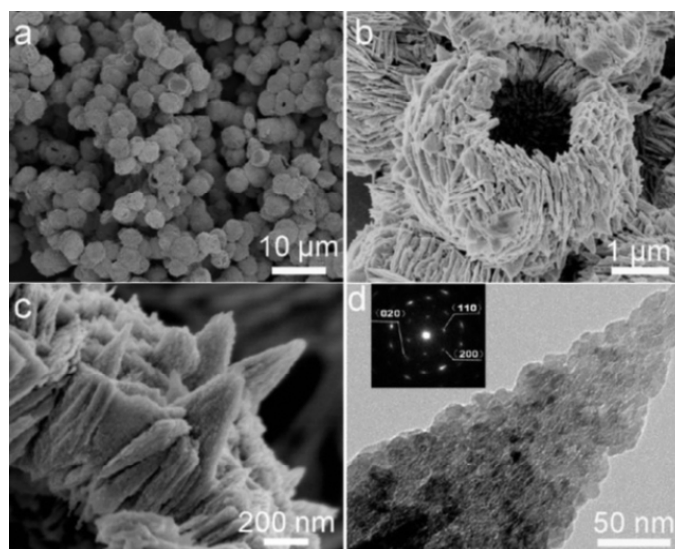


Fig. 41. Images of hierarchical porous spherical particles CuO. (a, b) SEM image of CuO particles; (c) an image of the wall structure of CuO particles; (d) TEM image of a nanoplate from a CuO particle. Reprinted with permission from Ref. [69]; Copyright 2012 American Chemical Society.

The growth mechanism through “oriented attachment” and Ostwald’s mechanism was proposed to explain the formation of hierarchical structure and pores in CuO particles. The former plays a role in the formation of primary micro- and mesopores, while the other plays a role in further enlargement of the pores.

The authors noted that CuO particles give excellent sensory properties (high sensitivity, rapid response and

recovery) due to their structure with open macropores. Such spherical particles can also be useful in applications such as solar cells, lithium batteries, photocatalysis, where kinetics of diffusion plays an important role.

A hydrothermal method for manufacturing CuO microspheres in the presence of ethylene glycol was demonstrated in [70] (Fig. 43). The reaction temperature, its duration and the amount of reagents had a sig-

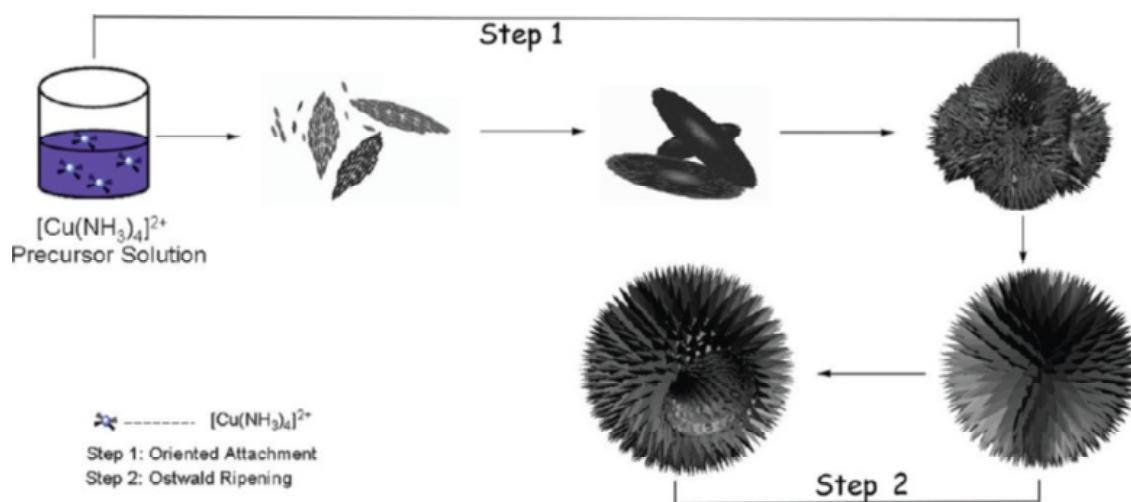


Fig. 42. Schematic illustration of the process of formation of a hierarchical structure and pores in CuO particles. Reprinted with permission from Ref. [69]; Copyright 2012 American Chemical Society.

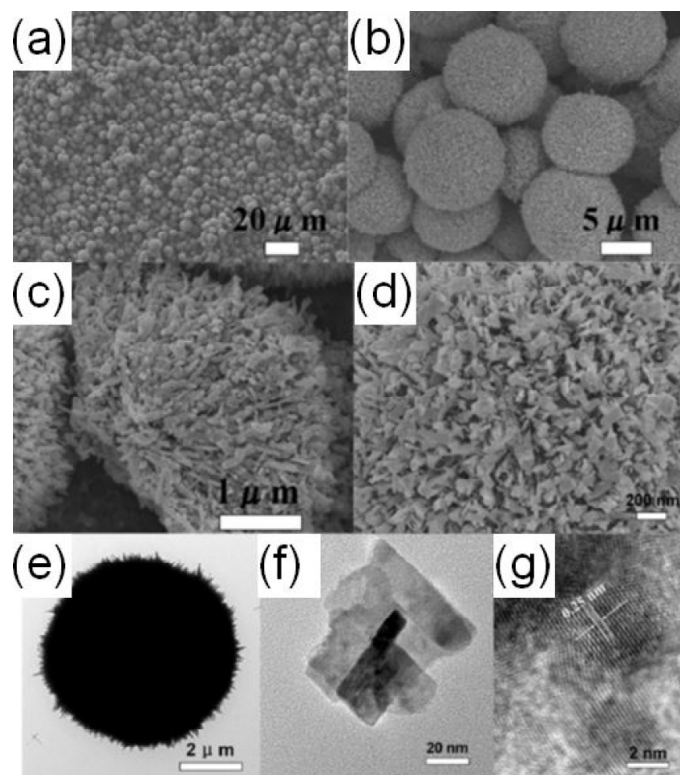


Fig. 43. Characterization of hierarchical structures of CuO: (a, b) images of SEM of various magnifications, (c) SEM image of internal structure, (d) SEM image of surface structure, (e) TEM image of a separate microsphere, (f) and (g) a high resolution TEM image at the edge of the CuO nanowire. Used with permission of Royal Society of Chemistry, from Ref. [70]; permission conveyed through Copyright Clearance Center, Inc.

nificant effect on the morphology and structure of the particles. The CuO microspheres were obtained over a wide range of reaction conditions and contained nanosheets (Fig. 44), had a surface area of 10.6-57.5 m²/g and a diameter of 3-6 micrometers. It has been found that an increase in the amount of ethylene glycol from 0 to 12 ml results in a continuous increase in the specific surface area of CuO microspheres. The authors pointed to the potential applications for catalysts based on par-

ticle data in the field of organic synthesis. It was shown that in the catalytic reaction the Si conversion increased with the surface area of the CuO samples.

A method for obtaining hollow nanocubes of Cu₂O with a narrow size distribution by hydrolysis was demonstrated in [71] (Figs. 45 and 46). During this one-vessel process, the micro-powder CuCl was first dissolved in aqueous HCl with a very low pH, then the CuCl nanocubes were precipitated by the addition of pure

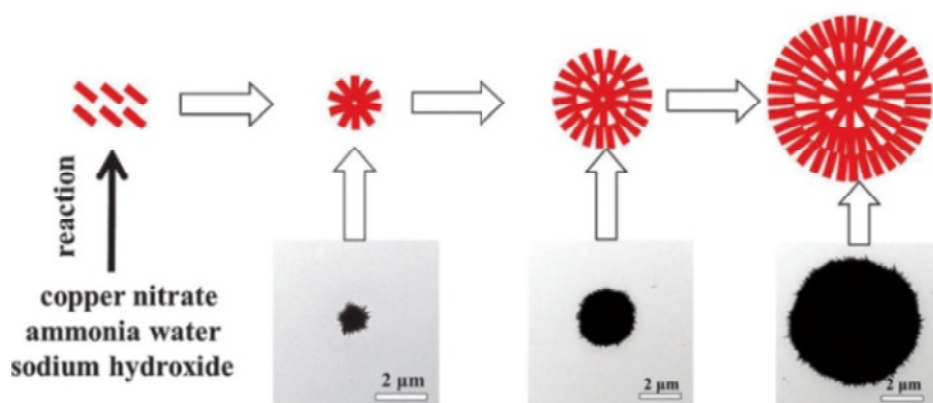


Fig. 44. Proposed process of formation of hierarchical microspheres of CuO consisting of nanobands. Used with permission of Royal Society of Chemistry, from Ref. [70]; permission conveyed through Copyright Clearance Center, Inc.

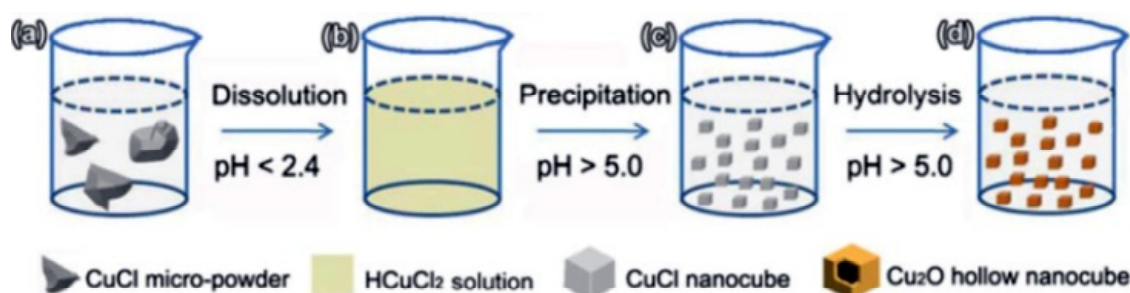


Fig. 45. Schematic illustration of a single-vessel synthesis of hollow nanocubes Cu_2O from a micro powder CuCl. Used with permission of Royal Society of Chemistry, from Ref. [71]; permission conveyed through Copyright Clearance Center, Inc.

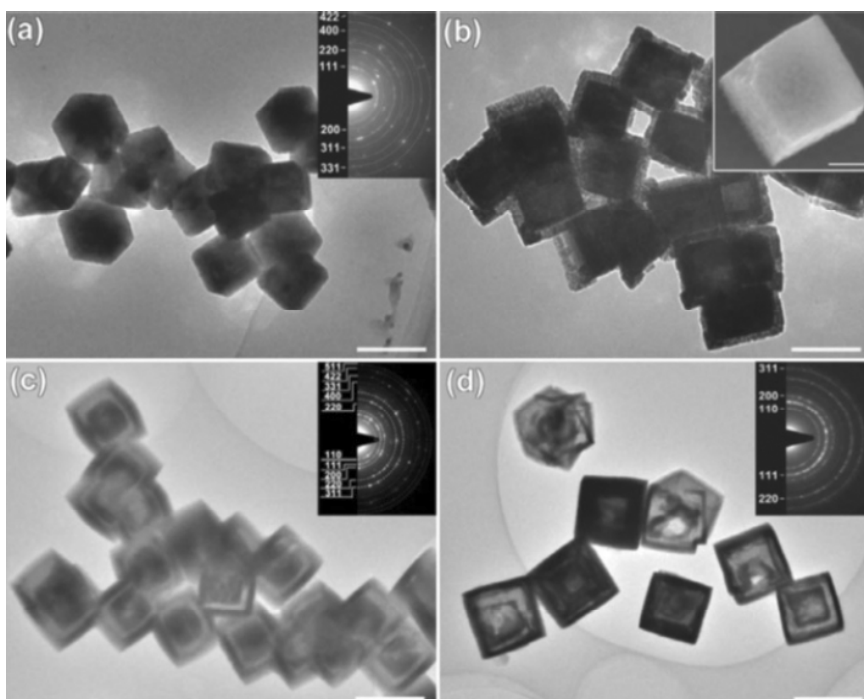


Fig. 46. TEM images showing the gradual conversion of CuCl nanocubes into hollow nanocubes of Cu_2O at pH 6.5. The time evolution is shown: 0 (a), 10 (b), 20 (c), and 30 min. (d). The scalebars are 200 nm, except for the insertion on (b), where the SEM image is given with a scalebar of 100 nm. Used with permission of Royal Society of Chemistry, from Ref. [71]; permission conveyed through Copyright Clearance Center, Inc.

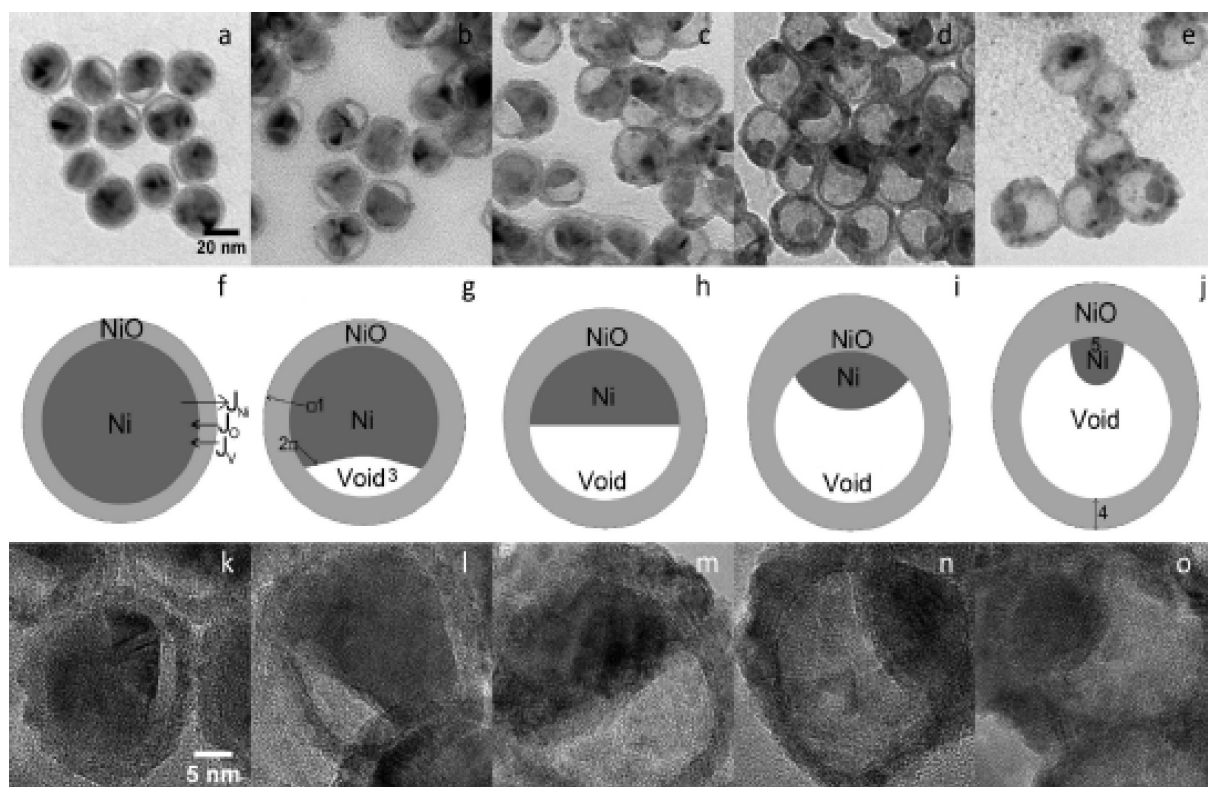


Fig. 47. TEM images of 26 nm nanoparticles after oxidation in air at 300 °C for (a) 90, (b) 120, (c) 150, (d) 180, and (e) 210 min. Corresponding oxidation schemes and high-resolution TEM images are shown below (a - e). (g - j) (1) Nickel diffuses across the Ni/NiO interface only and (2) vacancies are injected at the interface and diffuse to the void. (3) The void nucleates when vacancies supersaturate. (4) The shell remains the same thickness where the void nucleated, because little lateral Ni diffusion occurs along the void/shell interface or in the NiO shell. (5) Toward the end of oxidation, the core becomes a small ball whose oxidation might be slowed by the reduced Ni/NiO interfacial area and the thick NiO layer through which Ni cations must diffuse. Reprinted with permission from Ref. [73]; Copyright (2010) American Chemical Society.

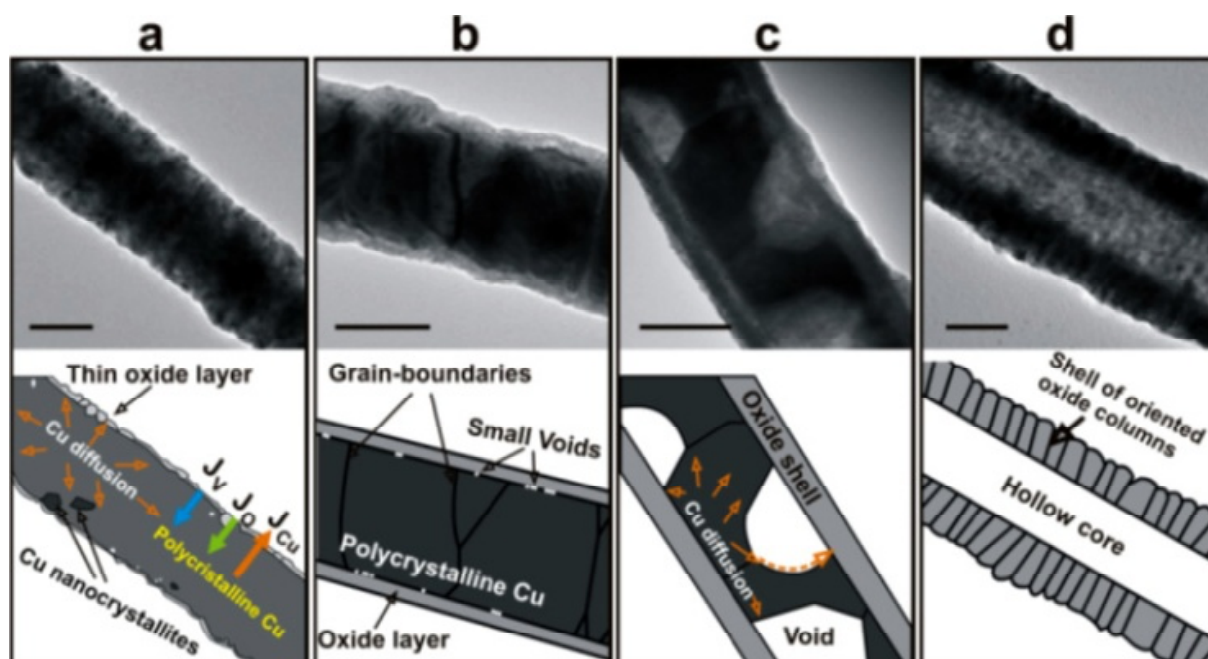


Fig. 48. TEM images and corresponding illustrations showing the evolution of Cu nanowire during thermal oxidation in air at 300 °C. The oxidation time was varied: (a) 1 min., (B) 2 min., (C) 3 min., and (d) 4 min. The scalebar is 100 nm. Reprinted with permission from Ref. [74]; Copyright (2013) John Wiley and Sons.

water and raising the pH to 6.5. At the last stage, CuCl nanocubes gradually reacted with water, resulting in uniform hollow nanocubes of Cu_2O as a result of complete hydrolysis. This work demonstrates for the first time the method of synthesis of hollow nanocubes Cu_2O without reducing agents or surfactants.

In the review article [72] and the original work [73] the mechanism of formation of internal cavities in particles is examined in detail on the basis of the latest experimental data. In particular, for example of nickel nanoparticles, a possibility of forming an asymmetric cavity is indicated (Fig. 47). It was observed that the oxide shell of the particle is thinner on the side where there is a large cavity (Fig. 47). The formation of one large cavity may be more favourable compared to multiple small cavities, as in the case of a symmetrical mechanism. This can be reasoned by the fact that the surface energy of many small cavities is higher than the surface energy of one large cavity.

As indicated in Ref. [74], the formation of pores in nanowires can be described in a similar manner (see Fig. 48). The transformation process starts with adsorption of oxygen to the outer side of the metallic nanowire, leading to a thin layer of metal oxide (see Fig. 48a). After forming a core-shell type structure, the metal ions diffuse through the oxide layer, reaching the outer surface. Simultaneously, the oxygen adsorbed on the outside of the wire diffuses through the oxide layer and penetrates to the metal core.

For some metals, such as Co, Cu, Fe, and Ni, the diffusion coefficient of metallic ions through their own oxides is much higher than the diffusion coefficient of oxygen ions. This fact leads to the formation of a multiple supersaturated vacancy regions along the metal oxide interface, which subsequently condense, forming a number of separate small cavities in the metallic core. Fusion of cavities is the final mechanism leading to hollow oxide nanostructures (Figs. 48 and 49).

5.1. Formation of cavity and growth of oxide whiskers from copper particles

An original and simple method of obtaining an array of oxide whiskers is described, for example in [75-77], annealing in air a copper substrate at temperatures up to 450 °C. As shown in [27], a large contribution to the mechanism of formation and growth of whiskers during such annealing is made by the defective structure of the substrate. There is a number of scientific papers on the mechanisms of growth [22,77] and properties of the whiskers obtained [77]. However, little information is given on structural-phase transformations in the copper substrate itself, which proceed simultaneously with growth on the surface of whiskers.

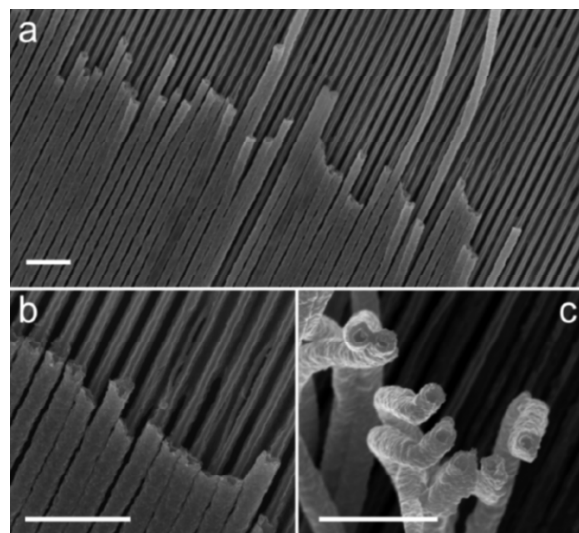


Fig. 49. (a, b) SEM images showing nanotubes of copper oxide fabricated on a lattice silicon substrate by thermal oxidation of copper nanowires for 1 hour at 300 °C. (C) SEM image of copper oxide nanotubes separated from the substrate. Scalebars are 1 micrometer. Reprinted with permission from Ref. [74]; Copyright (2013) John Wiley and Sons.

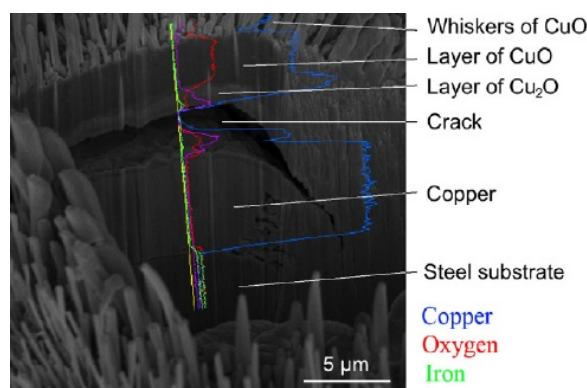


Fig. 50. Scheme of multilayer structure of oxidized copper coating. Reprinted from Ref. [78]; Copyright (2015), with permission from Elsevier.

As is known, annealing of copper in the presence of oxygen is accompanied by an oxidative reaction. According to the Cu- O_2 state diagram, two stable copper oxides are possible: copper (I) Cu_2O oxide having a red color and copper (II) oxide CuO are black.

Copper oxidation processes are a long-standing problem in such branches of science as chemistry, physics and metallurgy. At present, a number of models and theories have been proposed on this subject - a two-layer oxidation model is classical. The complexity of the problem of oxidation of materials is the relationship between chemical oxidation processes at the atomic level, the diffusion of atoms within the material and the strong heterogeneity of the oxidized region, often leading to the formation of internal stresses and structural defects.

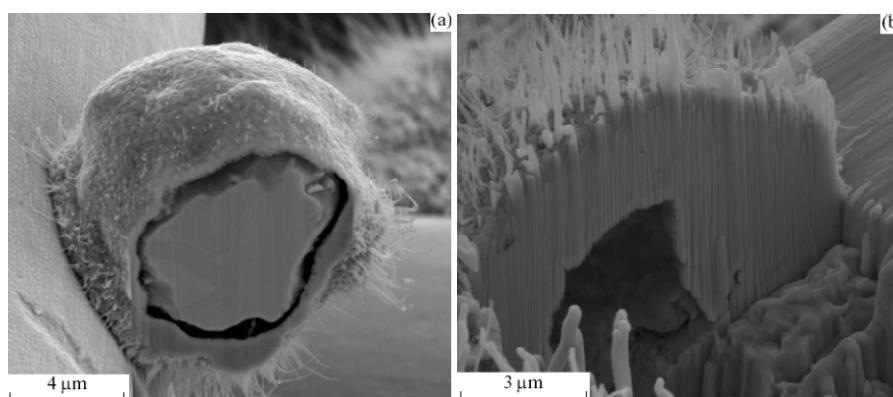


Fig. 51. Internal multilayer structure of oxidized copper particles with a cavity and a metal core (a) and without an inner core. Reprinted from Ref. [79], with permission © Allerton Press, Inc., 2015.

However, despite all the successes in this area, some aspects of the problem remain open. For example, in [74,77,78] it is reported that during the annealing of copper in air, a porous structure, a “forest” of whiskers on the surface, cavities in microparticles and cracks in continuous coatings are formed (Fig. 50). As was shown in the annealing and cutting experiments of oxidized copper particles (see Ref. [79]), an internal cavity appears in them, and a metallic core can also be present (Fig. 51). Formation of a multilayer structure with a cavity during annealing of a copper coating and particles still lacks an accurate theoretical explanation.

5.2. Model of oxidation of copper particles under annealing

Let us outline a qualitative model of cavity formation and related structural transformations in small copper particles under annealing. Phase and structural transformations in small copper particles during annealing can be presented as a sequence:

1. **The initial stage of heating.** The copper particle undergoes heating in the environment of gaseous oxygen. The increased temperature activates the volumetric and diffusion surfaces in copper and the relaxation processes in the nonequilibrium defective structure of the particle.
2. **The initial oxidation stage.** There is a rapid formation of a near-surface oxidized Cu_2O layer in the presence of a direct gas-particle separation.
3. **The stage of rapid oxidation.** The growth of the Cu_2O phase continues through the active diffusion of copper atoms in the bulk of the particle and over the surface of the oxidized Cu_2O layer. This process is much more intense than the diffusion of oxygen into the interior of the particle (the Kirkendall effect). In particular, this is due to the high concentration of internal defects in the copper particle and the presence of mechanical stresses

in it. In this case, the formation of Cu_2O islands and a nanoporous structure inside the copper core occurs. The most likely explanation for the appearance of defects in the form of nanopores is the action of the vacancy mechanism. As a result of that mechanism, nanopores are formed from vacancy disks, followed by the growth of nanopores due to a vacancy outflow [25]. Because of the high rate of oxidation compared to the rate of relaxation processes in the Cu_2O phase, it is fixed in the form of a brittle nanoporous layer. According to [25], in the process of annealing from nonequilibrium vacancies, porous channels can be formed. The formation of porous channels and their observation were reported in [80]. The mechanism of formation of porous channels was considered in detail in [25].

4. **The stage of slow oxidation.** The diffusion flux of copper atoms from the core slows down as nonequilibrium defects are exhausted. This activates the secondary oxidation of the Cu_2O layer and the growth of the CuO phase. The high stresses caused by the large difference in lattice parameters and the Pilling-Bedworth ratio (the volume of oxide referred to the volume of the metal from which it was obtained) lead to interfacial stratification and the formation of internal cavities. At the same time, there is a formation of growth centers for whiskers in the vicinity of places with easy transport of copper, i.e. porous channels. The movement of copper atoms to the surface (to the growth centers of whiskers) leads to a reduction in the copper base adherently bonded to the oxide layer, causing compression stresses in the plane of the oxide layer and tensile stresses of the normal copper surface. These compressive stresses can relax through the formation of the cavity through a crack. Further growth of the cavity can occur due to the surface diffusion of copper atoms along the core and further in the porous channels, which allows one to explain the occurrence of in-

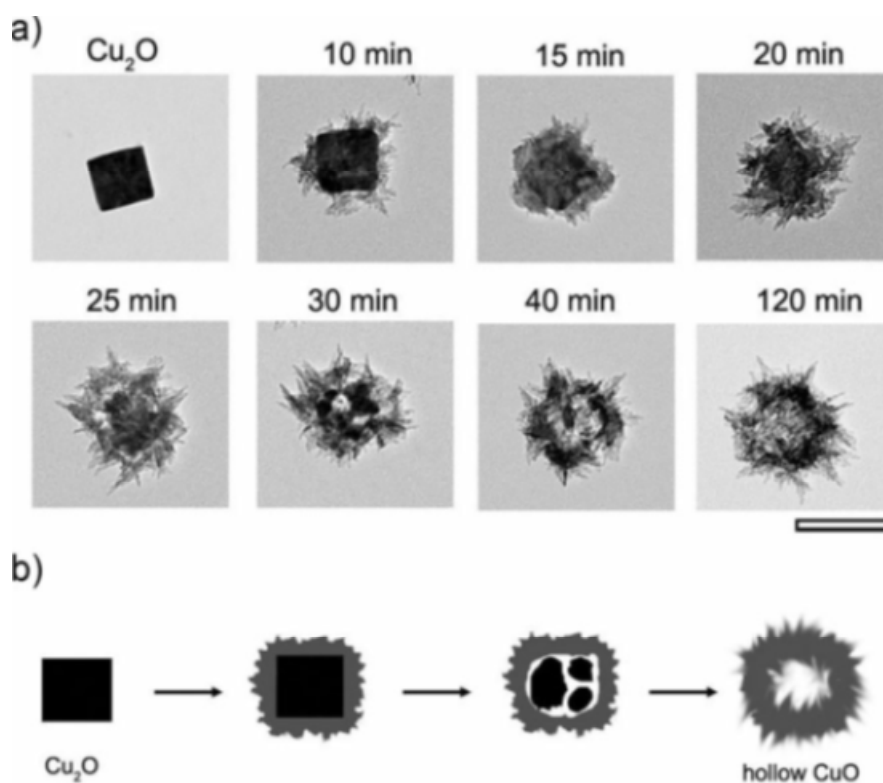


Fig. 52. The process of oxidation of Cu_2O nanocubes: a) TEM images, b) structural transformation scheme. Reprinted with permission from Ref. [81]; Copyright (2009) John Wiley and Sons.

ternal cavities comparable in volume with the copper core (Fig. 51).

5.3. Applications of small particles with developed surface

A number of works have shown the potential use of nanoparticles with a developed surface as materials for lithium batteries. For example, the synthesis of nanocubes Cu_2O was shown in [81] (Fig. 52). Controllable oxidation of Cu_2O nanocubes led to the formation of hollow cubes of CuO , hollow spheres, and hedgehog-like particles through a sequential deposition process. The hedgehog-like CuO particles showed excellent electrochemical characteristics for lithium batteries in comparison with other nanostructures. Precise control over the morphology of oxide nanoparticles would serve as the basis for improving the properties of lithium batteries. The authors point out the importance of experiments with other oxides, such as FeO , CoO , and Co_3O_4 in achieving this goal.

In [92] porous hollow octahedral CuO particles (Fig. 53) were synthesized by a hydrothermal method and subsequent thermal decomposition at $300\text{ }^\circ\text{C}$ (Fig. 54). Such particles were tested as electrodes in lithium batteries and showed very stable cyclic properties and speed.

6. SUMMARY AND CONCLUSIONS

Since the 40s of the 20th century, whiskers of tin, cadmium, silver, copper oxide, as well as other metals and non-metallic compounds have been discovered and characterized under various conditions. The practically important task of suppressing the growth of tin whiskers in the coatings of electrical contacts was solved by involving a toxic element - lead, which puts on the agenda the search for an alternative solution. On the other hand, the growing needs of the economy make it necessary to seek ways to control the growth of whiskers in order to use them for various industrial needs.

Several concepts and models of growth whiskers were proposed on the basis of various methodological approaches: dislocation models, models of recrystallization, diffusion models. However, at present no convincing and general model has been proposed to explain the growth of whiskers under given conditions and the internal structure of whiskers. Hopefully, the development of such a model is a matter of the near future.

In the end we would like to emphasize some general conclusions about the mechanisms of growth of metal and oxide whiskers:

1. The presence and distribution of *mechanical stresses* in the layers of material creates a driving force for the growth of whiskers.

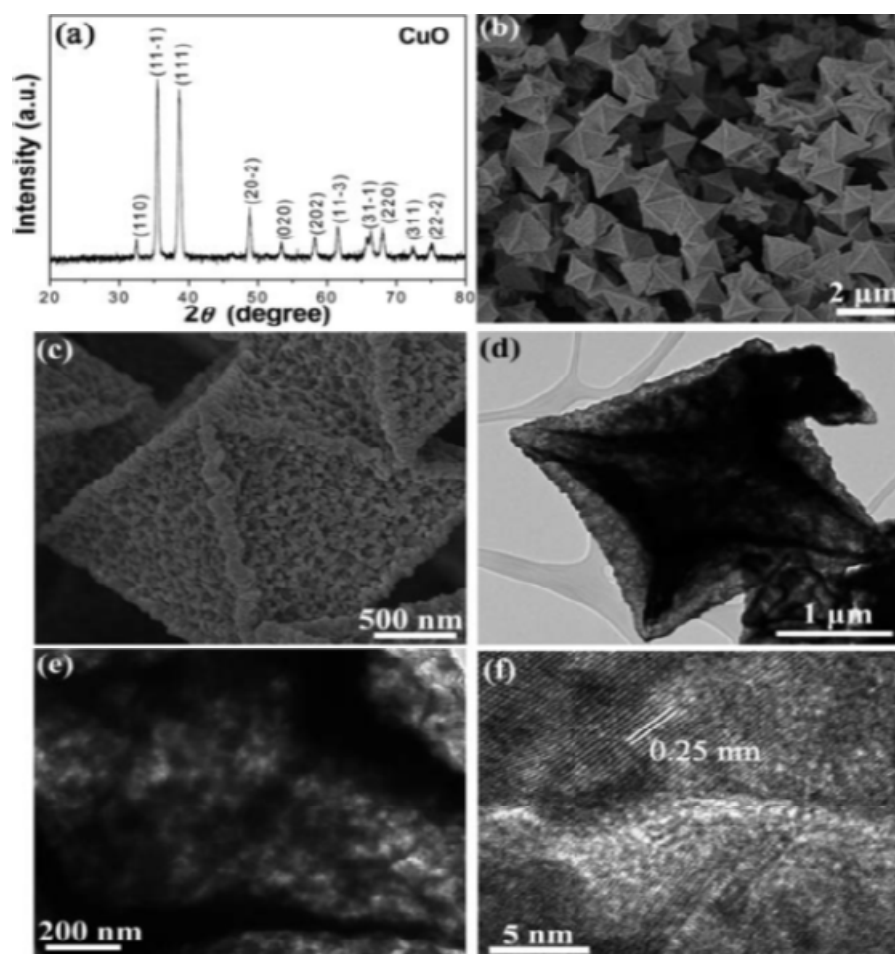


Fig. 53. Hollow octahedral CuO particles: (a) the x-ray diffraction pattern, (b) and (c) SEM images, (d) and (e) TEM images, and (f) high-resolution TEM image. Reprinted with permission from Ref. [82]; Copyright (2013) Royal Society of Chemistry.

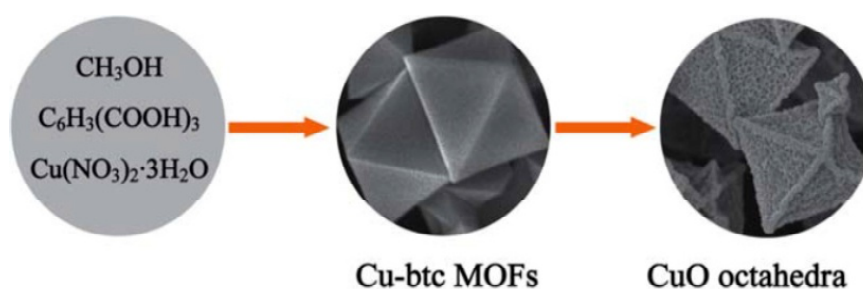


Fig. 54. Schematic illustration of the formation of hollow octahedral CuO particles. Reprinted with permission from Ref. [82]; Copyright (2013) Royal Society of Chemistry.

2. Mechanical stresses in metal coatings of tin on a copper base (and other coatings with metal whiskers) can be caused by a reaction to form intermetallic compounds between them. In the case of composite coatings, the stress source can be formed already in the process of their formation. For a copper base during annealing in air, the source of mechanical stresses can be the interaction of oxidized Cu_2O , CuO layers and the copper base itself.

3. The structure of the coating with grains of different orientations and the geometry of the boundaries can

create conditions for the motion of atoms as a material for the whisker by means of recrystallization and diffusion.

4. A *protective layer* on the surface of metals (for example, oxide coating in the case of tin) can serve to preserve mechanical stresses inside the coating, otherwise able to relax them through structural changes without ejecting the whisker.

In the course of this review, metal oxide whiskers and associated structural transformations at the micro-/nanoscale were also tackled. In particular, the problem

of oxidation of a copper coating and particles from electrolytic copper during annealing in air is described in connection to its potential applications. It is shown that in this case a complex multilayer multiphase structure is formed. Porous channels and internal stresses in oxide layers facilitate the diffusion of copper, the growth of whiskers, and the formation of such defects as macropores and cracks. Diffusion-chemical structural transformations and thermal action lead to mechanical tensile stresses and subsequent phase separation through a crack.

From the point of view of academic research, it appears helpful to elaborate on the role of the Kirkendall effect in the formation of cavities. For example, it would be possible to do this by computer simulation methods, but it should be noted that currently proposed models [83-85] are limited to modeling the basic mechanisms of cavity formation. Molecular dynamic simulations, would be useful for explaining complex phenomena found experimentally, such as the formation of asymmetric hollow nanospheres, segmented and bamboo-like nanotubes [72]. Finally, understanding the fundamental mechanisms of the structure of small particles will serve as the basis for the new applications in environmental and energy technologies.

ACKNOWLEDGEMENTS

The authors gratefully acknowledge financial support of the Russian Science Foundation under Grant 19–72–30004.

REFERENCES

- [1] H. L. Cobb, Cadmium whiskers, *Monthly Rev. Am. Electroplaters Soc.*, 1946, vol. 33, no. 28, pp. 28-30.
- [2] K. G. Compton, A. Mendizza, and S. M. Arnold, *Filamentary Growth on Metal Surfaces-Whiskers*, Corrosion, 1951, vol. 7, no. 10, p. 327-334, <https://doi.org/10.5006/0010-9312-7.10.327>
- [3] C. Herring and J. K. Galt, *Elastic and Plastic Properties of Very Small Metal Specimens*, *Phys. Rev.*, 1952, vol. 85, no. 6, p. 1060. <https://doi.org/10.1103/PhysRev.85.1060.2>
- [4] J. Smetana, *Theory of Tin Whisker Growth: 'The End Game'*, *IEEE Trans. Electron. Packag. Manuf.*, 2007, vol. 30., no. 1., pp. 11-22. <https://doi.org/10.1109/TEPM.2006.890645>
- [5] W. Bevis Hutchinson, James Oliver, Margareta Nylen, and Joacim Hagstrom, *Whisker Growth from Tin Coatings*, *Materials Science Forum*, Trans Tech Publications, Ltd., Oct. 2004, vol. 467-470, pp. 465-470, <https://doi.org/10.4028/www.scientific.net/MSF.467-470.465>
- [6] M. Umalas, S. Vlassov, B. Polyakov, L. M. Dorogin, R. Saar, I. Kink, R. Löhmus, A. Löhmus, and A. E. Romanov, *Electron beam induced growth of silver nanowhiskers*, unpublished.
- [7] M. O. Peach, *Mechanism of growth of whiskers on cadmium*, *J. Appl. Phys.*, 1952, vol. 23, no. 12, pp. 1401-1403, 1952. <https://doi.org/10.1063/1.1702147>
- [8] J. D. Eshelby, *A tentative theory of metallic whisker growth*, *Phys. Rev.*, 1953, vol. 91, no. 3, pp. 755-756. <https://doi.org/10.1103/PhysRev.91.755.2>
- [9] U. Lindborg, *A model for the spontaneous growth of Zn, cadmium, and tin whiskers*, *Acta Metallur.*, 1976, vol. 24, no. 2, pp. 181-186. [https://doi.org/10.1016/0001-6160\(76\)90021-3](https://doi.org/10.1016/0001-6160(76)90021-3)
- [10] A. E. Romanov, A. A. Vikarchuk, A. L. Kolesnikova, L. M. Dorogin, I. Kink, and E. C. Aifantis, *Structural transformations in nano- and microobjects triggered by disclinations*, *J. Mater. Res.*, 2012, vol. 27, no. 3, pp. 545-551. <https://doi.org/10.1557/jmr.2011.372>
- [11] A. E. Romanov, L. M. Dorogin, A. L. Kolesnikova, I. Kink, I. S. Yasnikov, and A. A. Vikarchuk, *A Model of Whisker Crystal Growth from a Pentagonal Small Particle*, *Technical Physics Letters*, 2014, vol. 40, pp. 174-176. <https://doi.org/10.1134/S1063785014020266>
- [12] K. Tu and J. Li, *Spontaneous whisker growth on lead-free solder finishes*, *Materials Science and Engineering: A*, 2005, vol. 409, no. 1, pp. 131-139. <https://doi.org/10.1016/j.msea.2005.06.074>
- [13] E. A. Gulbransen, T. P. Copan, and K. F. Andrew, *Oxidation of Copper between 250 and 450 C and the Growth of CuO "Whiskers"*, *J. Electrochem. Soc.*, 1961, vol. 108, no. 2, pp. 119-123. <https://doi.org/10.1149/1.2428024>
- [14] X. Jiang, T. Herricks, and Y. Xia, *CuO Nanowires Can be Synthesized by Heating Copper Substrates in Air*, *Nano Lett.*, 2002, vol. 2, no. 12, p. 1333-1339. <https://doi.org/10.1021/nl0257519>
- [15] N. Mukherjee, B. Show, S. K. Maji, U. Madhu, S. K. Bhar, B. Ch. Mitra, G. G. Khan, and A. Mondal, *CuO nano-whiskers: Electrodeposition, Raman analysis, photoluminescence study and photocatalytic activity*, *Mater. Lett.*, 2011, vol. 65, no. 21-22, p. 3248-3250. <https://doi.org/10.1016/j.matlet.2011.07.016>
- [16] N.V. Sibirev, V.G. Dubrovskii, G.E. Cirilin, V.A. Egorov, Yu.B. Samsonenko, and V.M. Ustinov, *Deposition-Rate Dependence of the Height of GaAs-Nanowires*, *Semiconductors*, 2008, vol. 42,

- no. 11, p. 1259-1263. <https://doi.org/10.1134/S106378260811002X>
- [17] H. Johnson, *Rollback the Lead-Free Initiative*, High-Speed Digital Design Online Newsletter, vol. 10, no. 01, 2007. http://www.sigcon.com/Pubs/news/10_01.htm
- [18] H. L. Reynolds and R. Hilty, *Investigations of Zinc (Zn) Whiskers using FIB Technology*, IPC/JEDEC Lead Free North America Conference (Boston, MA), 2004. <https://pdfs.semanticscholar.org/7d45/67bb784d9b5786fa89b1f6bec73d46744fcd.pdf>
- [19] Y.-T. Cheng, A. M. Weiner, C. A. Wong, M. P. Balogh, and M. J. Lukitsch, *Stress-induced growth of bismuth nanowires*, Appl. Phys. Lett., 2002, vol. 81, no. 17, pp. 3248–3250. <https://doi.org/10.1063/1.1515885>.
- [20] B. H. Chudnovsky, *Degradation of Power Contacts in Industrial Atmosphere: Silver Corrosion and Whiskers*, Proceedings of the Forty-Eighth IEEE Holm Conference on Electrical Contacts, Orlando, FL, USA, 2002, pp. 140-150. <https://ieeexplore.ieee.org/document/1040834>
- [21] M. Chen, Y. Yue, and Y. Ju, *Growth of metal and metal oxide nanowires driven by the stress-induced migration*, J. Appl. Phys., 2012, vol. 111, no. 10, pp. 104305-1–104305-6. <https://doi.org/10.1063/1.4718436>
- [22] I. S. Yasnikov and A. A. Vikarchuk, *Mechanisms of Relaxation of Elastic Stresses in the Process of Growth of Nanoparticles and Microcrystals with Disclination Defects in Electrocrystallization of FCC Metals*, Metal Science and Heat Treatment, 2007, vol. 49, pp. 97-104. <https://doi.org/10.1007/s11041-007-0018-5>
- [23] G. Pfefferkorn, *Elektronenmikroskopische Untersuchungen über den Oxydationsvorgang von Metallen*, Naturwiss., 1953, vol. 40, pp. 551-552. <https://doi.org/10.1007/BF00639678>
- [24] P. Shao, Sh. Deng, J. Chen, and N. Xu, *Large-scale fabrication of ordered arrays of microcontainers and the restraint effect on growth of CuO nanowires*, Nanoscale Res. Lett., 2011, vol. 7:86. <https://doi.org/10.1186/1556-276X-6-86>
- [25] A.A. Vikarchuk and M.V. Dorogov, *Features of the evolution of the structure and morphology of the surface of icosahedral copper particles in the annealing process*, JETP Letters, 2013, vol. 97, pp. 594-598. <https://doi.org/10.1134/S0021364013100111>
- [26] W. Zhang, X. Wen, and Sh. Yang, *Controlled Reactions on a Copper Surface: Synthesis and Characterization of Nanostructured Copper Compound Films*, Inorg. Chem., 2003, vol. 42, no. 16, pp. 5005-5014. <https://doi.org/10.1021/ic0344214>
- [27] O. V. Kharissova and B. I. Kharisov, *Less-Common Nanostructures in the Forms of Vegetation*, Ind. Eng. Chem. Res., 2010, vol. 49, no. 22, p. 11142-11169. <https://doi.org/10.1021/ie1017139>
- [28] S. E. Koonce and S. M. Arnold, *Growth of Metal Whiskers*, J. Appl. Phys., 1953, vol. 24, no. 3, pp. 365-366. <https://doi.org/10.1063/1.1721283>
- [29] M. Kaur, K. P. Muthe, S. K. Deshpande, Sh. Choudhury, J. B. Singh, N. Verma, S. K. Gupta, and J. V. Yakhmi, *Growth and branching of CuO nanowires by thermal oxidation of copper*, J. Cryst. Growth, 2006, vol. 289, no. 2, pp. 670-675. <https://doi.org/10.1016/j.jcrysgro.2005.11.111>
- [30] F.C. Frank, *Crystal growth and dislocations*, Adv. in Phys., 1952, vol. 1, no. 1, p. 91-109. <https://doi.org/10.1080/00018735200101171>
- [31] S. M. Arnold, *The Growth and Properties of Metal Whiskers*, Proc. 43rd Annual Convention of the American Electroplaters' Soc., 1956, p. 26.
- [32] V.K. Glazunova and N.T. Kudravtsev, *An investigation of the conditions of spontaneous growth of filiform crystals on electrolytic coatings*, Journal of Applied Chemistry, 1963, vol. 36, p. 543.
- [33] J. C.-B. Lee, Y.-L. Yao, F.-Y. Chiang, P. J. Zheng, C. C. Liao, and Y. S. Chou, *Characterization study of lead-free SnCu plated packages*, n Proceedings of the 52nd Electronic Components and Technology Conference, San Diego, Calif, USA, May 2002, pp. 1238–1245.
- [34] J. B. LeBret and M. G. Norton, *Electron microscopy study of tin whisker growth*, J. Mater. Res., 2003, vol. 18, no. 3, pp. 585-593. <https://doi.org/10.1557/JMR.2003.0076>
- [35] M. Rozen, *Practical whisker growth control methods*, Plating, 1968, vol. 55, no. 11, pp. 1155-1168.
- [36] N. A. J. Sabbagh and E. H. J. McQueen, *Tin whiskers: Causes and remedies*, Metal Finishing, March 1975, pp. 27-31.
- [37] S. C. Britton, *Spontaneous growth of whiskers on tin coatings: 20 years of observation*, Trans. Inst. Metal Finishing, 1974, vol. 52, no. 3, pp. 95-105.
- [38] K. N. Tu, *Irreversible processes of spontaneous whisker growth in bimetallic Cu-Sn thin reactions*, Phys. Rev. B, 1994, vol. 49, no. 3, pp. 2030-2034. <https://doi.org/10.1103/PhysRevB.49.2030>

- [39] B. Z. Lee and D. N. Lee, *Spontaneous growth mechanism of tin whiskers*, *Acta Metallurgica*, 1998, vol. 46, no. 10, pp. 3701-3714. [https://doi.org/10.1016/S1359-6454\(98\)00045-7](https://doi.org/10.1016/S1359-6454(98)00045-7)
- [40] K. Whitlaw and J. Crosby, *An empirical study into whisker-growth of tin and tin alloy electrodeposits*, *Proc. 2002 AESF SUR/FIN Conf.*, 2002, pp. 19-30.
- [41] N. Vo, Y. Nadaira, T. Matsura, M. Tsuruya, R. Kangas, J. Conrad, B. Sundram, K. Lee, and S. Arunasalam, *Pb-free plating for peripheral/leadframe packages*, *Proc. IEEE Electronic Components and Technology Conf.*, 2001, pp. 213-218. http://thor.inemi.org/webdownload/projects/ese/Vo_IEEE.pdf
- [42] N. Vo and M. Tsuruya, *Whisker assessment of tin-based finishes for leadframe packages*, *Proc. ECO Design Japan Symp.*, 2002, p. 120.
- [43] M. Dittes, P. Oberndorff, and L. Petit, *Tin whisker formation-results, test methods, and countermeasures*, *Proc. IEEE Electronic Components Technology Conf.*, 2003, pp. 822-826.
- [44] D. W. Romm, D. C. Abbott, S. Grenney, and M. Khan, *Whisker Evaluation of Tin-Plated Logic Component Leads*, Texas Instruments Application Report, SZZA037A, February 2003. https://www.psm.com/HTML/FILES/forums/leadfree/ti_article_sn_plating.pdf
- [45] A. Y. Kozlov, M. V. Dorogov, N. V. Chirkunova, I. M. Sosnin, A. A. Vikarchuk, and A. E. Romanov, *CuO Nanowhiskers-Based Photocatalysts for Wastewater Treatment*, *Nano Hybrids and Composites*, 2017, vol. 13, pp. 183-189. <https://doi.org/10.4028/www.scientific.net/nhc.13.183>
- [46] T. Homma and S. Issiki, *Role of CuO whisker growth in the oxidation kinetics of pure copper*, *Acta Metall.*, 1964, vol. 12, no. 9, pp. 1092-1093. [https://doi.org/10.1016/0001-6160\(64\)90082-3](https://doi.org/10.1016/0001-6160(64)90082-3)
- [47] A. Kumar, A. K. Srivastava, P. Tiwari and R. V. Nandedkar, *The effect of growth parameters on the aspect ratio and number density of CuO nanorods*, *J. Phys.: Condens. Matter*, 2004, vol. 16, no. 47, pp. 8531-8543, 2004. <https://doi.org/10.1088/0953-8984/16/47/007>
- [48] S. E. Koonce and S. M. Arnold, *Metal whiskers*, *J. Appl. Phys.*, 1954, vol. 25, no. 1, pp. 134-135. <https://doi.org/10.1063/1.1721508>
- [49] G. S. Baker, *Angular Bends in Whiskers*, *Acta Metall.*, 1957, vol. 5, no. 7, p. 353-357. [https://doi.org/10.1016/0001-6160\(57\)90001-9](https://doi.org/10.1016/0001-6160(57)90001-9)
- [50] D. F. Susan, J. R. Michael, W. G. Yelton, B. B. McKenzie, R. P. Grant, J. Pillars, and M. A. Rodriguez, *Understanding and Predicting Metallic Whisker Growth and its Effects on Reliability: LDRD Final Report*, Sandia National Laboratories Report, SAND2012-0519, 2012. <https://prod-ng.sandia.gov/techlib-noauth/access-control.cgi/2012/120519.pdf>
- [51] L. Yuan, Y. Wang, R. Mema, and G. Zhou, *Driving force and growth mechanism for spontaneous oxide nanowire formation during the thermal oxidation of metals*, *Acta Mater.*, 2011, vol. 59, pp. 2491-2500. <https://doi.org/10.1016/j.actamat.2010.12.052>
- [52] M. Dorogov, A. Kalmykov, L. Sorokin, A. Kozlov, A. Myasoedov, D. Kirilenko, N. Chirkunova, A. Priezzheva, A. Romanov, and E. C. Aifantis, *CuO nanowhiskers: preparation, structure features, properties, and applications*, *Materials Science and Technology*, 2018, vol. 34, no. 17, pp. 2126-2135. <https://doi.org/10.1080/02670836.2018.1514706>
- [53] H. P. Howard, J. Cheng, P. T. Vianco, and J. C. M. Li, *Interface flow mechanism for tin whisker growth*, *Acta Mater.*, 2011, vol. 59, no. 5, p. 1957-1963. <https://doi.org/10.1016/j.actamat.2010.11.061>
- [54] G. Galyon, *Whisker Formation Concepts—The End Game*, *IEEE Trans. Comp., Pack. Manufact. Technology*, 2011, vol. 1, no. 7, pp. 1098-1109.
- [55] M. W. Barsoum, E. N. Hoffman, R. D. Doherty, S. Gupta, and A. Zavaliangos, *Driving Force and Mechanism for Spontaneous Metal Whisker Formation*, *Phys. Rev. Lett.*, 2004, vol. 93, no. 20, p. 206104-1. <https://doi.org/10.1103/PhysRevLett.93.206104>
- [56] A. Egli, *Tin Deposit Ripening and Whisker Growth*, oral talk in ECTC 2005 (Orlando), May 2005.
- [57] G. T. Galyon and L. Palmer, *An Integrated Theory of Whisker Formation: The Physical Metallurgy of Whisker Formation and the Role of Internal Stresses*, *IEEE Trans. Electr. Pack. Manufact.*, 2005, vol. 28, no. 1, pp. 17-30. <https://doi.org/10.1109/TEPM.2005.847443>
- [58] T. Shibutani, Q. Yu, T. Yamashita, and M. Shiratori, *Stress-Induced Tin Whisker Initiation Under Contact Loading*, *IEEE Trans. Electr. Pack. Manufact.*, 2006, vol. 29, no. 4, pp. 259-264. <https://doi.org/10.1109/TEPM.2006.887357>
- [59] M. O. Peach, *Mechanism of growth of whiskers on cadmium*, *J. Appl. Phys.*, 1952, vol. 23, no. 12, pp. 1401-1403. <https://doi.org/10.1063/1.1702147>
- [60] W. C. Dash, *Generation of Prismatic Dislocation Loops in Silicon Crystals*, *Phys. Rev. Lett.*, 1958,

- vol. 1, no. 11, pp. 400-402. <https://doi.org/10.1103/PhysRevLett.1.400>
- [61] J.-H. Zhao, P. Su, M. Ding, Sh. Chopin, and P. S. Ho, *Microstructure-Based Stress Modeling of Tin Whisker Growth*, IEEE Trans. Electr. Pack. Manufact., 2006, vol. 29, no. 4, pp. 265-273. <https://www.me.utexas.edu/~ho/papers/EPM2006.pdf>
- [62] E. Buchovecky, N. Jadhav, A. F. Bower, and E. Chason, *Finite Element Modeling of Stress Evolution in Sn Films due to Growth of the Cu₆Sn₅ Intermetallic Compound*, J. Electr. Mater., 2009, vol. 38, no. 12, pp. 2676-2684. <https://doi.org/10.1007/s11664-009-0911-3>
- [63] E. J. Buchovecky, N. Du, and A. F. Bower, *A model of Sn whisker growth by coupled plastic flow and grain boundary diffusion*, Appl. Phys. Lett., 2009, vol. 94, no. 19, p. 191904-1 - 191904-3. <https://doi.org/10.1063/1.3136865>
- [64] J. J. Teo, Yu Change, and H. Ch. Zeng, *Fabrications of Hollow Nanocubes of Cu₂O and Cu via Reductive Self-Assembly of CuO Nanocrystals*, Langmuir, 2006, vol. 22, no. 17, pp. 7369-7377. <https://doi.org/10.1021/la060439q>
- [65] J. Hong, J. Li, Y. Ni, *Urchin-like CuO microspheres: Synthesis, characterization, and properties*, Journal of Alloys and Compounds, 2009, vol. 481, no. 1-2, pp. 610-615. <https://doi.org/10.1016/j.jallcom.2009.03.043>
- [66] A.A. Vikarchuk, N. Gryznova, O. Dovzhenko, M.V. Dorogov, and A.E. Romanov, *Structural Phase Transformations and Morphological Changes of Icosahedral Small Copper Particles in Temperature Fields and Reactive Media*, Advanced Materials Research, 2014, vol. 1013, pp. 205-210. <https://doi.org/10.4028/www.scientific.net/amr.1013.205>
- [67] C. J. Love, J. D. Smith, Y. Cui, and K. K. Varanasi, *Size-dependent thermal oxidation of copper: single-step synthesis of hierarchical nanostructures*, Nanoscale, 2011, vol. 3, pp. 4972-4976. <https://doi.org/10.1039/C1NR10993F>
- [68] Z. Guo, M.-L. Seol, M.-S. Kim, J.-H. Ahn, Y.-K. Choi, J.-H. Liub and X.-J. Huang, *Hollow CuO nanospheres uniformly anchored on porous Si nanowires: preparation and their potential use as electrochemical sensors*, Nanoscale, 2012, vol. 4, no. 23, pp. 7525-7531. <https://doi.org/10.1039/c2nr32556j>
- [69] Y. Qin, F. Zhang, Y. Chen, Y. Zhou, J. Li, A. Zhu, Y. Luo, Y. Tian, and J. Yang, *Hierarchically Porous CuO Hollow Spheres Fabricated via a One-Pot Template-Free Method for High-Performance Gas Sensors*, Journal of Physical Chemistry C, 2012, vol. 116, no. 22, pp. 11994-12000. <https://doi.org/10.1021/jp212029n>
- [70] Z. Zhang, H. Che, Y. Wang, L. Song, Z. Zhong, and F. Su, *Preparation of hierarchical dandelion-like CuO microspheres with enhanced catalytic performance for dimethyldichlorosilane synthesis*, Catalysis Science & Technology, 2012, vol. 2, pp. 1953-1960. <https://doi.org/10.1039/C2CY20199B>
- [71] H. Liu, Y. Zhou, S. A. Kulinich, J.-J. Li, L.-L. Han, Sh.-Zh. Qiao, and X.-W. Du, *Scalable synthesis of hollow Cu₂O nanocubes with unique optical properties via a simple hydrolysis-based approach*, Journal of Materials Chemistry A, 2013, vol. 1, pp. 302-307. <https://doi.org/10.1039/C2TA00138A>
- [72] A. A. E. Mel, R. Nakamura and C. Bittencourt, *The Kirkendall effect and nanoscience: hollow nanospheres and nanotubes*, Beilstein Journal of Nanotechnology, 2015, vol. 6, pp. 1348-1361. <https://doi.org/10.3762/bjnano.6.139>
- [73] J.G. Railsback, A.C. Johnston-Peck, J. Wang, and J.B. Tracy, *Size-dependent nanoscale kirkendall effect during the oxidation of nickel nanoparticles*, ACS Nano, 2010, vol. 4, no. 4, pp. 1913-1920. <https://doi.org/10.1021/nn901736y>
- [74] A. El Mel, M. Buffière, P. Tessier, S. Konstantinidis, W. Xu, K. Du, I. Wathuthanthri, C. Choi, C. Bittencourt, and R. Snyders, *Highly ordered hollow oxide nanostructures: The kirkendall effect at the nanoscale*, Small, 2013, vol. 9, no. 17, pp. 2838-2843. <https://doi.org/10.1002/sml.201202824>
- [75] E.A. Gulbransen, T.P. Copan, and K.F. Andrew, *Oxidation of copper between 250 ° and 450 °C and the growth of CuO "whiskers"*, J. Electrochem. Soc., 1961, vol. 108, no. 2, pp. 119-123. <https://doi.org/10.1149/1.2428024>
- [76] S. Rackauskas, A.G. Nasibulin, H. Jiang, Y. Tian, V.I. Kleshch, J. Sainio, E.D. Obraztsova, S.N. Bokova, A.N. Obraztsov, and E.I. Kauppinen, *A novel method for metal oxide nanowire synthesis*, Nanotechnol., 2009, vol. 20, no. 16, pp. 165603-1-165603-8. <https://doi.org/10.1088/0957-4484/20/16/165603>
- [77] A.N. Abramova, M.V. Dorogov, S. Vlassov, I. Kink, L.M. Dorogin, R. Löhms, A.E. Romanov, and A.A. Vikarchuk, *Nanowhisker of copper oxide: fabrication technique, structural features and mechanical properties*, Mater. Phys. Mech., 2014, vol. 19, no. 1, pp. 88-95, 2014. http://www.ipme.ru/e-journals/MPM/no_11914/MPM119_08_abramova.pdf

- [78] M.V. Dorogov, A.N. Priezheva, S. Vlassov, I. Kink, E. Shulga, L.M. Dorogin, R. Löhmus, M.N. Tyurkov, A.A. Vikarchuk, and A.E. Romanov, *Phase and structural transformations in annealed copper coatings in relation to oxide whisker growth*, Applied Surface Science, 2013, vol. 346, p. 423-427. <https://doi.org/10.1016/j.apsusc.2015.03.211>
- [79] A.N. Priezheva, M.V. Dorogov, M.N. Tyurkov, S. Vlassov, E. Shulga, R. Löhmus, L.M. Dorogin, I. Kink, D.L. Merson, A.A. Vikarchuk, and A.E. Romanov, *Phase transformations in icosahedral small copper particles during their annealing in different gas media*, Bulletin of the Russian Academy of Sciences. Physics, 2015, vol. 79, p. 1098-11100. <https://doi.org/10.3103/S1062873815090154>
- [80] J.-H. Park and K. Natesan, *Oxidation of copper and electronic transport in copper oxides*, Oxid. Met., 1993, vol. 39, pp. 411-435. <https://doi.org/10.1007/BF00664664>
- [81] J. C. Park, J. Kim, H. Kwon, and H. Song, *Gram-Scale Synthesis of Cu₂O Nanocubes and Subsequent Oxidation to CuO Hollow Nanostructures for Lithium-Ion Battery Anode*, Materials, Advanced Materials, 2009, vol. 21, no. 7, pp. 803-807. <https://doi.org/10.1002/adma.200800596>
- [82] R. Wu, X. Qian, F. Yu, H. Liu, K. Zhou, J. Wei, and Y. Huang, *MOF-templated formation of porous CuO hollow octahedra for lithium-ion battery anode materials*, Journal of Materials Chemistry A, 2013, vol. 1, p. 11126-11129. <https://doi.org/10.1039/C3TA12621H>
- [83] S. Jana, J. W. Chang, and R. M. Rioux, *Synthesis and Modeling of Hollow Intermetallic Ni-Zn Nanoparticles Formed by the Kirkendall Effect*, Nano Letters, 2013, vol.13, no. 8, pp. 3618-3625. <https://doi.org/10.1021/nl401467r>
- [84] L. Klinger, O. Kraft, and E. Rabkin, *A model of Kirkendall hollowing of core-shell nanowires and nanoparticles controlled by short-circuit diffusion*, Acta Mater., 2015, vol. 83, pp. 180-186, 2015. <https://doi.org/10.1016/j.actamat.2014.09.050>
- [85] K. N. Tu and U. Gösele, *Hollow nanostructures based on the Kirkendall effect: Design and stability considerations*, Applied Physics Letters, 2005, vol. 86, no. 9, pp. 093111-1 - 093111-3. <https://doi.org/10.1063/1.1873044>